Journal of Vertebrate Paleontology
Publication details, including instructions for authors and subscription information:
http://www.informaworld.com/smpp/title~content=t917000010

A basal coelurosaur (Dinosauria: Theropoda) from the Late Jurassic (Oxfordian) of the Shishugou Formation in Wucaiwan, People's Republic of China

Jonah N. Choiniere[a]; James M. Clark[a]; Catherine A. Forster[a]; Xing Xu[b]
[a] Department of Biological Sciences, The George Washington University, Washington, D.C., U.S.A. [b] Institute of Vertebrate Paleontology and Paleoanthropology, Beijing, China

Online publication date: 02 December 2010

To cite this Article Choiniere, Jonah N. , Clark, James M. , Forster, Catherine A. and Xu, Xing(2010) 'A basal coelurosaur (Dinosauria: Theropoda) from the Late Jurassic (Oxfordian) of the Shishugou Formation in Wucaiwan, People's Republic of China', Journal of Vertebrate Paleontology, 30: 6, 1773 — 1796
To link to this Article: DOI: 10.1080/02724634.2010.520779
URL: http://dx.doi.org/10.1080/02724634.2010.520779

Journal of Vertebrate Paleontology 30(6):1773–1796, November 2010

ARTICLE

A BASAL COELUROSAUR (DINOSAURIA: THEROPODA) FROM THE LATE JURASSIC (OXFORDIAN) OF THE SHISHUGOU FORMATION IN WUCAIWAN, PEOPLE'S REPUBLIC OF CHINA

JONAH N. CHOINIERE,*[1] JAMES M. CLARK,[1] CATHERINE A. FORSTER,[1] and XING XU[2]
[1]The George Washington University, Department of Biological Sciences, Washington, D.C. 20052, U.S.A., jchoiniere@amnh.org;
[2]Institute of Vertebrate Paleontology and Paleoanthropology, Beijing 100044, China

ABSTRACT—We describe a new coelurosaurian theropod, *Zuolong salleei*, gen. et sp. nov., from exposures of the upper part of the Shishugou Formation at the Wucaiwan locality, Xinjiang Autonomous Region, People's Republic of China. *Zuolong* has a large, inclined quadrate foramen that extends onto the medial surface of the quadratojugal, an unusually large fovea capitis on the femoral head, and an apomorphically large distal condyle of metatarsal III with a medially projecting flange on the extensor surface. Radiometric dating of the Shishugou Formation constrains the age of the specimen to the beginning of the Late Jurassic (Oxfordian). A cladistic analysis of *Zuolong salleei* in a broadly sampled theropod data matrix recovers it as a basal coelurosaur. These data make *Zuolong* one of the oldest coelurosaur fossils yet known that preserves both cranial and postcranial bones.

INTRODUCTION

The Shishugou Formation, exposed in the Junggar Basin north of the Tian Shan in the Xinjiang Autonomous Region, People's Republic of China, has a history of fossil collecting dating back to the Sino-Swedish expedition led by Sven Hedin in 1928 (Hedin, 1931; Young, 1937). Two large-bodied theropods were collected from the Shishugou Formation at Jiangjunmiao: the basal tetanuran *Monolophosaurus jiangi* (Zhao and Currie, 1994), collected by Chinese expeditions (Dong, 1994); and the allosauroid *Sinraptor dongi* (Currie and Zhao, 1994), collected by the Chinese-Canadian Dinosaur Project in the late 1980s (Dong, 1994; Grady, 1993). Recently, excavations made by the Sino-American field expedition in the Shishugou Formation at the Wucaiwan locality have produced a number of dinosaur fossils, including several species of small- to medium-bodied theropod (Clark et al., 2006a,b; Xu et al., 2006). We describe here a new coelurosaurian theropod from the upper part of the Middle to Upper Jurassic Shishugou Formation, which is a thick sedimentary group of interbedded sandstones, conglomerates, and paleosols (Eberth et al., 2001). The new species, discovered by the Sino-American field expedition in 2001, is known from several cranial bones and a disarticulated postcranial skeleton (Figs. 1–17).

Coelurosaurians older than the Kimmeridgian stage of the Late Jurassic are relatively rare, but recent discoveries of new taxa and phylogenetic analysis strongly support initial coelurosaurian diversification by the Middle Jurassic, and the diversification of derived coelurosaurian groups by the earliest Late Jurassic. The Middle Jurassic *Proceratosaurus*, known from a partial skull and mandible, has recently been recognized as a basal tyrannosauroid (Rauhut and Milner, 2008; Rauhut et al., 2009), and it was previously recovered as a basal coelurosaur (Rauhut, 2003). Results of radiometric dating of the Daohugou sediments that produced the maniraptorans *Pedopenna* (Xu and Zhang, 2005), *Epidendrosaurus* (Zhang et al., 2002), and *Epidexipteryx* (Zhang et al., 2008) are imprecise and debated: some studies suggest a range from 168 to 152 Ma (Liu et al., 2006), corresponding to the Bathonian–Kimmeridgian marine stages, but other studies suggest the Daohugou beds are Early Cretaceous in age (He et al., 2004). The troodontid *Anchiornis* (Hu et al., 2009) is known from the Tiaojishan Formation, which is more precisely dated at 161–151 Ma (Xu et al., 2003). The identification of the Early Jurassic *Eshanosaurus deguchiianus* as a therizinosauroid (Xu et al., 2001) remains tentative until more complete material is found and its age is now called into question (Barrett, 2009).

Institutional Abbreviations—**AMNH**, American Museum of Natural History, New York, New York, U.S.A.; **IGM**, Institute of Geology, Mongolian Academy of Sciences, Ulaanbaatar, Mongolia; **IVPP**, Institute for Vertebrate Paleontology and Paleoanthropology, Beijing, China; **LMNH**, The Natural History Museum, London, U.K.; **OUMNH**, Oxford University Museum of Natural History, Oxford, U.K.; **TPII**, Thanksgiving Point Institute, Provo, Utah, U.S.A.; **UMNH**, Utah Museum of Natural History, Salt Lake City, Utah, U.S.A.; **YPM**, Yale Peabody Museum, New Haven, Connecticut, U.S.A.

SYSTEMATIC PALEONTOLOGY

THEROPODA Marsh, 1881
TETANURAE Gauthier, 1986
COELUROSAURIA sensu Gauthier, 1986
ZUOLONG SALLEEI, gen. et sp. nov.
(Figs. 1–17)

Holotype—IVPP V15912, consisting of the following bones: left premaxilla; left maxilla; left quadrate; right and left quadratojugals; left squamosal; right and left ectopterygoids; left pterygoid; left lacrimal; partial frontal; partial parietal; left postorbital; one premaxillary and two maxillary or dentary teeth; five cervical, four dorsal, five sacral, and eight caudal vertebrae; right humerus; left radius and ulna; one complete manual ungual; left ilium; right and left pubes; right and left femora; right tibia;

*Corresponding author.

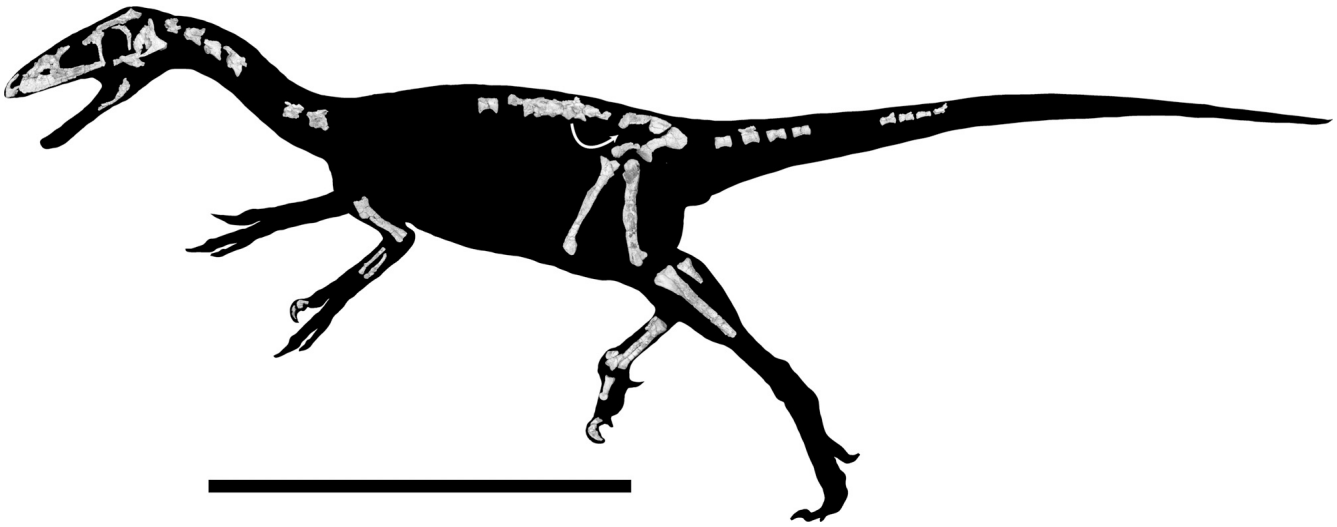

FIGURE 1. Skeletal map of *Zuolong salleei*. Scale bar equals 1 m.

proximal right fibula; right metatarsals II–IV; three pedal phalanges, pedal ungual.

Age and Distribution—Upper part of the Shishugou Formation, Wucaiwan, Xinjiang, People's Republic of China. Extensive 40Ar/39Ar dating of feldspars from intercalated tuffaceous layers of volcanic tuffs at Wucaiwan constrains the age of the specimen to between 158.7 ± 0.3 and 161.2 ± 0.2 Ma, approximately at the Oxfordian/Callovian boundary (Gradstein et al., 2004; Clark et al., 2006b). Because the holotype is from the upper part of the sediments between these dated tuffs, we consider the age of *Zuolong* to be Oxfordian.

Etymology—The generic name *Zuolong* refers to General Zuǒ Zōngtáng (also known as General Tso), who conquered portions of Xinjiang during the Qing dynasty, and the Chinese *long*, meaning dragon. The species epithet *salleei* is for Hilmar Sallee, whose bequest partially funded excavations at Wucaiwan.

Generic Diagnosis—As for the type and only species.

Diagnosis—Differs from all other theropods in possessing: large, slit-like quadrate foramen inclined medially at approximately 45° with associated deep fossa on the quadrate; sacral centrum 5 with an obliquely oriented posterior articular surface that is angled anterodorsally; fovea capitis very large, occupying almost the entire posterodorsal surface of the femoral head; distal condyle of metatarsal III large relative to that of other metatarsals and bearing an anteromedially projecting flange on its anteromedial margin. Differs from the co-occurring species *Guanlong wucaii* in having a square premaxillary body in lateral view; an external naris oriented at almost 45° to the horizontal; a triangular anterior end of the maxilla; an antorbital fossa that does not deeply emarginate the ascending process of the maxilla; a postorbital with frontal and jugal processes at right angles to each other; a short postacetabular wing of the ilium; and absence of a pubic tubercle. Differs from the basal coelurosaur *Tanycolagreus* in having a square, rather than rectangular, premaxillary body; a postorbital without an anterior process; a ventrally directed anterior process of the lacrimal; a straight ulna and radius; and a lateral ridge on cnemial crest of tibia. Differs from the basal coelurosaur *Coelurus* in having cervical vertebrae that lack paired lateral foramina and are not anteroposteriorly elongate; dorsal centra without a fossa on the lateral surface of the centrum; a straight, rather than sigmoidal, humeral shaft; a high and rounded, rather than low and squared, ilium; and a straight, rather than curved, femoral shaft.

DESCRIPTION

The disarticulated skeleton includes dermal skull bones and the quadrate, cervical, dorsal, sacral, and caudal vertebrae, and proximal forelimb and hindlimb bones (Figs. 1–17; Table 1). Notably missing are the braincase, most bones of the lower jaw, and the ischium.

Skull

Skull Openings—The external naris faces laterally. Its length is unknown, but unlike the enlarged, rectangular nares of *Guanlong* (Xu et al., 2006) and *Proceratosaurus* (Rauhut et al., 2009), the anterior end preserved on the premaxilla is short and rounded. The maxillary fenestra is small and the interfenestral pila is long. The maxillary fenestra is posteriorly displaced from the anterior margin of the antorbital fossa and located at mid-height of the maxilla. There is a small, deep depression located at the anteroventral corner of the antorbital fossa, in the location of the promaxillary foramen, but we cannot confirm that it pierces the maxilla, due to poor preservation in this region. The orbit is large, round, and laterally facing. The supratemporal fenestra was likely subcircular, based on the preserved border of this fenestra on the parietals, frontals, and postorbital. The infratemporal fenestra cannot be described because the jugal is not preserved.

Premaxilla—The left premaxilla (Fig. 2A, E, K) is missing the distal end of the maxillary process and a small portion of the distal tip of the palatal process. The body of the premaxilla is as long as it is high, as in *Proceratosaurus* (Rauhut et al., 2009) and unlike the dorsoventrally tall premaxillary body of *Tanycolagreus* (Carpenter et al., 2005a). The anterior and posterior surfaces of the bone both slant posterodorsally. The lateral surface of the nasal process of the premaxilla is convex. The maxillary process arches slightly dorsally beneath the nares, dorsoventrally constricting the anterior part of the narial opening. The posterior end of the lateral surface of the premaxilla is flat, unlike the condition in compsognathids (Peyer, 2006) and coelophysoids (Raath, 1977; Rauhut, 2003), where a low process originates on the posteroventral corner of the premaxillary body and extends posteriorly under the anterior end of the maxilla (Rauhut, 2003). A hatchet-shaped premaxillary palatal process extends posteromedially from the premaxillary body toward the palatal process of the maxilla. This palatal process is anteroposteriorly much shorter than that of *Duriavenator* (Benson, 2008b). The palatal

TABLE 1. Measurements (mm) of bones of *Zuolong salleei.*

Element	Measurement	Left	Right
Scapula	Length	173.8*	
Humerus	Length		155.4*
	Midshaft mediolateral width		13.8
	Midshaft anteroposterior breadth		22.3
	Minimum circumference		62.0
	Distal mediolateral width (across condyles)		41.0
	Distal anteroposterior breadth		15.0
Radius	Length	137.0	
	Midshaft mediolateral width	10.9	
	Midshaft anteroposterior breadth	12.8	
	Minimum circumference	42.5	
	Proximal mediolateral width	10.5	
	Proximal anteroposterior breadth	15.9	
	Distal mediolateral width	12.6	
	Distal anteroposterior breadth	20.3	
Ulna	Length	118.6	
	Midshaft mediolateral width	8.4	
	Midshaft anteroposterior breadth	13.3	
	Minimum circumference	38.2	
	Distal mediolateral width	9.6	
	Distal anteroposterior breadth	19.9	
Femur	Length	336.0	236.8*
	Midshaft mediolateral width	39.5	X
	Midshaft anteroposterior breadth	45.0	X
	Minimum circumference	112.3	X
	Proximal mediolateral width	66.3	X
	Proximal anteroposterior breadth (including femoral head)	32.2	X
	Distal mediolateral width	60.2	67.3
	Distal anteroposterior breadth (to posterior end of crista tibiofibularis	55.0	45.5*
Tibia	Length		273.2*
	Midshaft mediolateral width		36.2
	Midshaft anteroposterior breadth		28.5
	Minimum circumference		98.6
	Proximal mediolateral width		45.1
	Proximal anteroposterior breadth		69.7
Metatarsal II	Length	191.9	
	Midshaft mediolateral width	15.6	
	Midshaft anteroposterior breadth	18.1	
	Proximal mediolateral width	24.4	
	Proximal anteroposterior breadth	32.0	
	Distal mediolateral width	28.3	
	Distal anteroposterior breadth	24.4	
Metatarsal III	Length	224.3	
	Midshaft mediolateral width	16.2	
	Midshaft anteroposterior breadth	13.4	
	Proximal mediolateral width	23.0	
	Proximal anteroposterior breadth	42.9	
	Distal mediolateral width	37.7	
	Distal anteroposterior breadth	33.3	
Metatarsal IV	Length	201.7**	
	Proximal mediolateral width	20.3	
	Proximal anteroposterior breadth	38.0	
	Distal mediolateral width	23.2	
	Distal anteroposterior breadth	27.4	

Length measured in the same plane as the major axis of the bone.
*Measurement of preserved portion; **estimated measurement.

portion of the premaxilla is narrow, and an indentation along the midline indicates that the incisive foramen was large. In ventral view, the premaxillary symphysis is U-shaped. The roots of four teeth are present within rounded premaxillary alveoli, but the crowns are not preserved in situ. The first alveolus is smaller in diameter than the posterior three, which are subequal in size.

Maxilla—Small portions of the dorsoventrally low, triangular left maxilla are missing at the anterior contact with the premaxilla, along the posterior articulation with the jugal, and at the distal tip of the nasal ramus (Fig. 2B, F, J). The nasal ramus of the maxilla grades smoothly into the maxillary body at the anterior end, as in most coelurosaurians other than basal tyrannosauroids (Xu et al., 2006; Rauhut et al., 2009) and *Shuvuuia* (IGM 100/99). A small subnarial foramen is fully enclosed by the maxilla and located ventral to the anterior premaxillary-maxillary contact. A shallow groove on the anterior surface of the anterior end of the maxilla marks the premaxillary/maxillary contact. The posterior extent of this groove suggests that the maxillary process of the premaxilla was long and excluded the maxilla from participating in the external naris, as in a number of theropod taxa, including *Allosaurus* (Madsen, 1976), *Sinraptor* (Currie and Zhao, 1994), *Proceratosaurus* (LMNH R4860), *Ornitholestes* (AMNH 619), and dromaeosaurids (Norell and Makovicky, 2004), but differing from the conditions of *Monolophosaurus* (IVPP V84019), *Guanlong* (IVPP V14531 and V14532), coelophysoids, and abelisaurids (Rauhut, 2003). The antorbital fenestra and maxillary fenestra are located within a deeply recessed antorbital fossa. The antorbital fossa is ventrally bounded by a dorsoventrally low, laterally convex ridge that extends posteriorly from the anterior margin of the antorbital fossa along maxillary jugal ramus under most of the antorbital fenestra. This lateral ridge is situated ventral to the level of the dorsoventral midline of the jugal ramus. Numerous, shallow mental foramina are located just above the tooth row on the lateral surface of the maxilla. The alveolar margin is linear in lateral view. A narrow palatal process extends above the level of the tooth row along the entire length of the medial side of the jugal ramus of the maxilla. The anteromedial portion of the palatal process of the maxilla is medially expanded to contact the palatal process of the premaxilla. The narrow medial extension of the palatal process posterior to this junction indicates that the maxillary palate was not extensively developed.

There are 12 maxillary alveoli, and all the teeth are broken at the alveolar margin. The roots of maxillary teeth 2–7 are hourglass-shaped in cross-section, with median constrictions in ventral view. Unfused, polygonal interdental plates are present on the lingual alveolar margin. Unfused interdental plates are present in a variety of theropods, including *Syntarsus* (Raath, 1977), *Duriavenator* (Benson, 2008b), *Monolophosaurus* (Zhao and Currie, 1994), *Megalosaurus bucklandii* (Benson, 2009), *Tyrannosaurus* (Brochu, 2003), and *Guanlong* (IVPP V14531). In contrast, fusion of the interdental plates is common in ceratosaurs (e.g., *Masiakasaurus* [Carrano et al., 2002], *Majungasaurus* [Sampson and Witmer, 2007]), carcharodontosaurids (e.g., *Mapusaurus* [Coria and Currie, 2006], *Acrocanthosaurus* [Eddy, 2008a]), *Cryolophosaurus* (Smith et al., 2007), and *Allosaurus* (Madsen, 1976). The anterior-most preserved plate, between the second and third maxillary teeth, is almost square. The remaining interdental plates are subequal in size and pentagonal. The apex of the pentagon is ventrally directed and located in the gaps between adjacent teeth.

Lacrimal—The left lacrimal is poorly preserved but nearly complete (Fig. 2C, G, I). The bone is composed of an anteroventrally inclined maxillary process and a vertical jugal process, giving the lacrimal the shape of an inverted 'L.' The maxillary process is missing its anterior tip, and the jugal process is poorly preserved along the ventral margin at the jugal/maxillary contact. The junction of the maxillary and jugal processes forms the lacrimal angle, the lateral surface of which lacks a lacrimal foramen, although preservation in this region is poor. If a lacrimal foramen were present, it would most likely be small, as in many coelurosaurians such as *Tanycolagreus* (TPII 2000-09-29), rather than large, as in the non-coelurosaurian tetanurans *Sinraptor* (Currie and Zhao, 1994) and *Allosaurus* (Madsen, 1976). The lacrimal emargination for the antorbital fossa reaches almost to the posterodorsal margin of the lacrimal angle, forming a deep

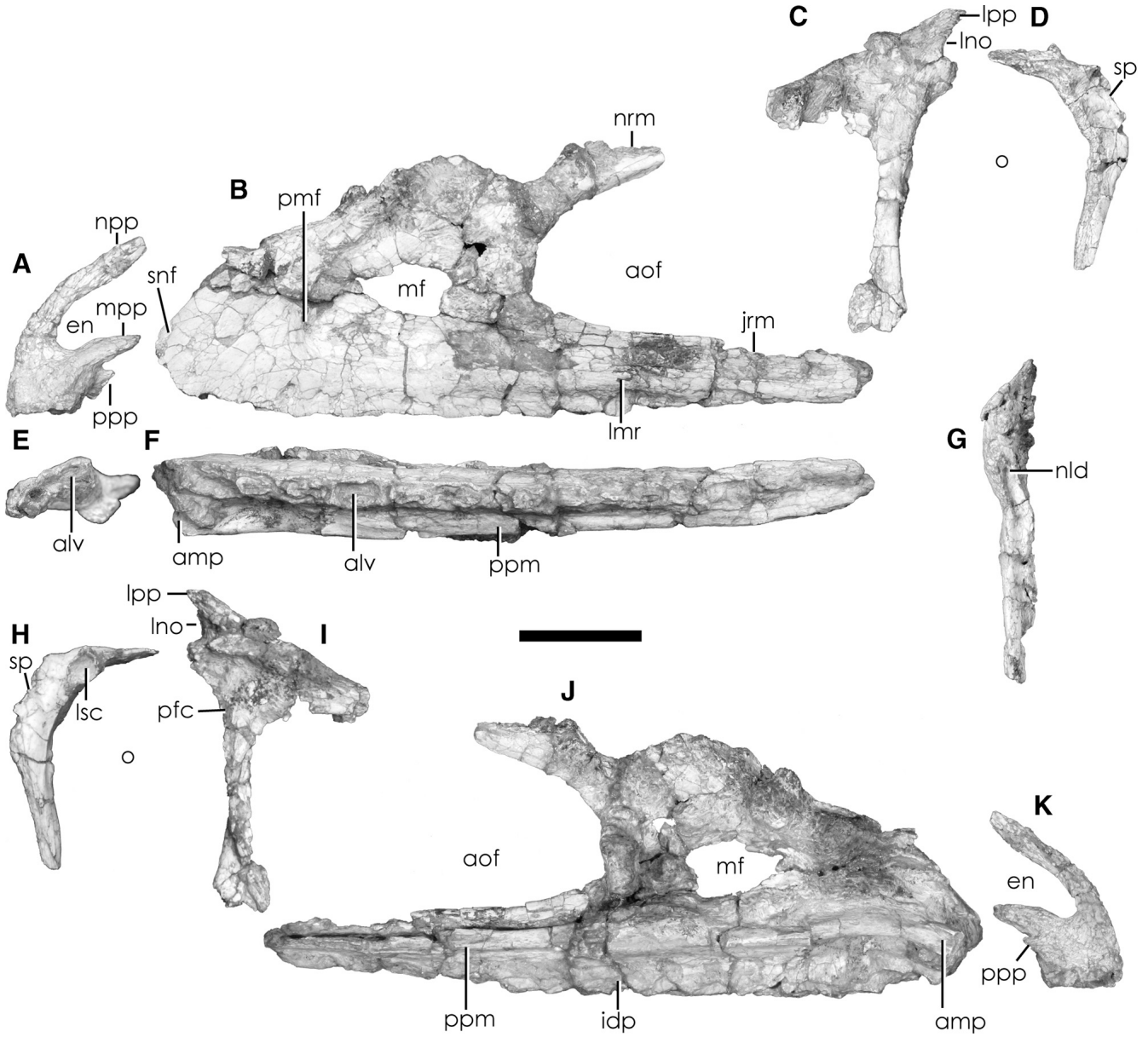

FIGURE 2. Craniodental bones of *Zuolong salleei*. **A**, left premaxilla in lateral view; **B**, left maxilla in lateral view; **C**, left lacrimal in lateral view; **D**, left postorbital in lateral view; **E**, left premaxilla in ventral view; **F**, left maxilla in ventral view; **G**, left lacrimal in posterior view; **H**, left postorbital in medial view; **I**, left lacrimal in medial view; **J**, left maxilla in medial view; **K**, left premaxilla in medial view. **Abbreviations**: **alv**, alveolus; **amp**, anteromedial process of maxillary palatal process; **aof**, antorbital fenestra; **en**, external naris; **idp**, interdental plate; **jrm**, jugal ramus of the maxilla; **lmr**, lateral maxillary ridge; **lno**, lacrimal notch; **lpp**, lacrimal posterior process; **lsc**, laterosphenoid contact; **mf**, maxillary foramen; **mpp**, maxillary process of the premaxilla; **nld**, nasolacrimal duct; **npp**, nasal process of the premaxilla; **nrm**, nasal ramus of the maxilla; **o**, orbit; **pmf**, promaxillary foramen; **pfc**, prefrontal contact; **ppm**, palatal process of maxilla; **ppp**, premaxillary palatal process; **snf**, subnarial foramen; **sp**, squamosal process. Scale bar equals 3 cm.

triangular pocket that opens anterolaterally and leaving only a thin lamina of bone at the posterior end of the lacrimal-nasal contact. Such an extensive antorbital fossa on the lacrimal is unknown in coelurosaurians, although the lacrimal angles of some oviraptorosaurs bear extensive pneumatization (Osmólska et al., 2004). The lacrimal angle of the allosauroid *Acrocanthosaurus* (Currie and Carpenter, 2000) is similarly emarginated by the antorbital fossa, but the lacrimal posterior and dorsal rims of the fossa are thick and rugose rather than thin and laminar. A deep pocket is present in this position in *Sinraptor* (Currie and Zhao, 1994) and *Allosaurus* (Madsen, 1976), but in these taxa the pocket is ovoid and recessed medially from the medial margin of the antorbital fossa (Currie and Zhao, 1994). The lacrimal lacks prominent lateral and dorsal rugosities, but a sharply pointed, posterodorsally directed process extends from the lacrimal angle and is indented on its posteroventral surface by a deep, posteriorly facing notch (Fig. 2C, I), a feature unknown in other coelurosaurians. It is likely that the notch at least partially articulated with a small prefrontal. A well-developed posterior notch is present in *Majungasaurus* (Sampson and Witmer, 2007)

and a weak notch is present in *Sinraptor* (Currie and Zhao, 1994), but in these taxa the notch is a result of the gap between the fused prefrontal and the suborbital process of the lacrimal rather than an articular surface for the prefrontal. Above the notch, the posterior surface of the posterodorsal process bears three small foramina. The medial surface of the lacrimal body is excavated by a triangular fossa extending from the antorbital fenestra to the orbit. The jugal process is straight and slender, lacking the pronounced anteroposterior expansion of the ventral end that is present in more primitive tetanurans, *Tanycolagreus*, and some tyrannosaurids (Holtz, 2004; Holtz et al., 2004; Carpenter et al., 2005a). The jugal process is composed of a laterally convex lateral lamina and an anteroposteriorly short medial lamina. The anterior margin of the lateral lamina is straight, as in *Tanycolagreus* (TPII 2000-09-29), whereas in many theropods, including *Sinovenator* (IVPP 10600), *Allosaurus* (Madsen, 1976), *Ornitholestes* (AMNH 619), and tyrannosauroids (Holtz, 2004), the lateral lamina is anteriorly convex in lateral view. The medial lamina is anteriorly concave in medial view. Dorsally, the two laminae meet at right angles along the posteromedial edge of the lateral lamina. Ventrally, the medial lamina curves anteriorly, and contacts the anteromedial edge of the lateral lamina at the ventral tip of the ventral process of the lacrimal. A small foramen marking the egress of the nasolacrimal duct pierces the posterior surface of the proximal portion of the jugal process. The anterior surface of the jugal process of the lacrimal is concave, forming the posterior edge of the antorbital fenestra. The posterior surface is shallowly concave, forming the anterior rim of the orbit. The medial surface of the medial lamina of the jugal process bears a shallow channel that marks the articular surface for the lacrimal process of the prefrontal.

Postorbital—The left postorbital is missing most of the squamosal process but is otherwise well preserved. It consists of a ventrally directed jugal process and an anteromedially directed frontal process (Fig. 2D, H). The lateral rim of the postorbital is thickened, projecting laterally above the orbit bears as a low, rugose ridge. The frontal process is dorsoventrally flattened and forms a dorsally concave, horizontal sheet at the dorsal margin of the orbit. The posterior margin of the dorsal surface is deeply excavated by the supratemporal fossa, which decreases in depth as it extends toward the anterior margin. On the medial surface of the frontal process, there is a cup-like laterosphenoid articular facet that lacks foramina on its medial surface. Although the laterosphenoid contact is infrequently preserved in theropod postorbitals, two small foramina are present on the laterosphenoid contact of *Majungasaurus* (Sampson and Witmer, 2007). Within Tetanurae, the laterosphenoid contact lacks foramina in both the relatively primitive *Eustreptospondylus* (Sadleir et al., 2008) and the relatively derived Deinonychus (Ostrom, 1969). In contrast, both *Allosaurus* (Madsen, 1976) and *Tyrannosaurus* (Brochu, 2003) have laterosphenoid contacts of the postorbital pneumatized by a series of small foramina on the medial surface. The jugal process of the postorbital tapers ventrally and is V-shaped in cross-section, with the 'V' opening posteriorly as a well-developed groove to accept the postorbital process of the jugal. The junction of the postorbital body and the base of the squamosal process is located dorsally, almost level with the frontal process. In derived coelurosaurians this junction is located more ventrally, at the midpoint of the descending jugal process.

Quadratojugal—The right quadratojugal is missing the anterior end of the jugal process and the dorsal end of the squamosal process. The left quadratojugal, which is complete and preserved in articulation with the left quadrate (Fig. 3A–D), consists of an anteriorly directed jugal process and an anteroposteriorly wide squamosal process that extensively contacts the lateral surface of the quadrate. These processes meet at the quadratojugal body at approximately a right angle. The jugal process tapers to a point anteriorly and is shallowly convex along its ventral margin. The ventral surface of the jugal process bears sutural marks that indicate that the ventral contact with the quadratojugal process of the jugal extended posteriorly to the level of the anterior margin of the squamosal process. The dorsal surface of the jugal

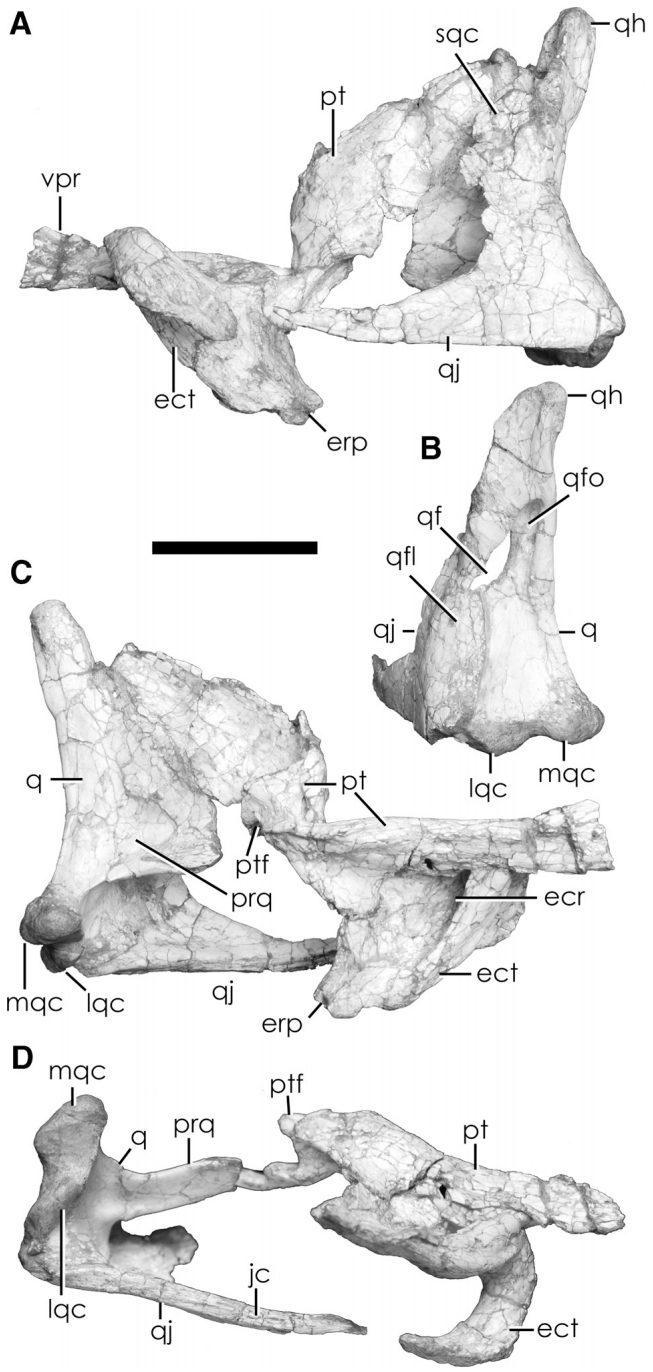

FIGURE 3. Craniodental bones of *Zuolong salleei*. Articulated left ectopterygoid, pterygoid, quadrate, and quadratojugal in **A**, lateral view; **B**, posterior view; **C**, medial view; **D**, ventral view. **Abbreviations**: **ecr**, ectopterygoid recess; **ect**, ectopterygoid; **erp**, ectopterygoid ramus of pterygoid; **jc**, jugal contact; **lqc**, lateral condyle of quadrate; **mqc**, medial condyle of quadrate; **prq**, pterygoid ramus of quadrate; **pt**, pterygoid; **ptf**, pterygoid flange; **q**, quadrate; **qf**, quadrate foramen; **qfl**, quadrate flange of quadratojugal; **qfo**, quadrate fossa; **qh**, quadrate head; **qj**, quadratojugal. Scale bar equals 3 cm.

process only bears a mediolaterally narrow sutural mark along the anterior end, indicating that the quadratojugal process of the jugal was bifid and asymmetrical posteriorly, with the dorsal portion shorter than the ventral portion. The jugal process has a wide ventral edge, with a low, hemicylindrical ridge visible in medial view that extends anteriorly from the lateral condyle of the quadrate to the anterior tip of the quadratojugal. The squamosal process extends dorsally three-quarters of the height of the quadrate and it contacts the quadratojugal process of the squamosal along its dorsal margin. The posterior edge of the quadratojugal is shallowly concave in lateral view. A tall, mediolaterally narrow posterior flange of the quadratojugal wraps around the lateral margin of the quadrate. This flange extends ventrally to the level of the lateral quadrate condyle and it extends dorsally to the dorsal level of the quadrate foramen. Although most of the quadrate foramen is bordered laterally by the quadrate, a small, V-shaped notch marking the ventrolateral tip of the quadrate foramen is present on the medial margin of the flange of the quadratojugal. A similarly tall flange (without the notch) is present in many tetanurans and some basal coelurosaurians, including *Sinraptor* (Currie and Zhao, 1994), *Allosaurus* (Eddy, 2008b), carcharodontosaurids (Eddy, 2008a, 2008b), and *Tanycolagreus* (Carpenter et al., 2005a). The posterior flange differs from the condition in most maniraptorans, where it extends posteriorly, rather than medially, as a dorsoventrally low, anteroposteriorly long tab (Norell and Makovicky, 1997; Osmólska et al., 2004). In *Ornitholestes* (AMNH 619), the tab is dorsoventrally short, but it is not as anteroposteriorly long as in other maniraptorans. In tyrannosauroids (Holtz, 2004), the quadratojugal has a flange similar to that of *Zuolong*, but the quadrate foramen is developed as a large opening between the quadrate and quadratojugal. Medially, the body of the quadratojugal is shallowly concave. The right quadratojugal bears two small foramina on the jugal process, located posteroventrally to the posteroventral corner of the infratemporal fenestra. These foramina are not present on the left quadratojugal.

Quadrate—The left quadrate is complete (Fig. 3A–C) and has no pneumatic openings in its cortical surface. In lateral view, the quadrate is shallowly concave posteriorly, so that the squamosal articulation is anterior to the mandibular articulation. The dorsal articular condyle for the squamosal is single-headed. The mandibular articular surface has two obliquely oriented condyles. The condyles are of similar mediolateral width, but the medial condyle is anteroposteriorly longer than the lateral condyle. The lateral margin of the lateral condyle is overlapped dorsolaterally by the posterior process of the quadratojugal. The pterygoid ramus of the quadrate is tall and approximately triangular in medial view. The pterygoid ramus has a shallow fossa located ventrally on its medial surface. There is also a shallow fossa located ventrally on the lateral surface that opens ventrolaterally and extends anteriorly from a point anterodorsal to the quadrate condyles. A mediolaterally narrow, hemicylindrical ridge runs along the posteromedial margin of the quadrate and is visible in posterior and medial views. This ridge is poorly developed ventrally, but it becomes more pronounced dorsally, terminating just ventral to the squamosal articulation. The mediolaterally wide, dorsoventrally short quadrate foramen is located at approximately the midpoint of the quadrate shaft. It is nearly surrounded by the quadrate and medially inclined at approximately 45° to the horizontal plane of the quadrate condyles. Medially, the quadrate foramen is located within a deeply excavated, triangular fossa on the medial edge of the quadrate. The medial border of this fossa is formed by the medial ridge on the quadrate shaft, and the dorsolateral border of the fossa is formed by an overhanging portion of the quadrate shaft. Fossae dorsal to the quadrate foramen are also present on the quadrate shafts of *Allosaurus*, *Sinraptor*, and carcharodontosaurids, but the fossae of carcharodontosaurids are pneumatic, forming deep blind cavities. Unlike the large quadrate foramen of *Zuolong*, in these taxa the quadrate foramina are generally small and subcircular (Eddy, 2008a). The large quadrate foramina of *Tyrannosaurus* (Brochu, 2003), *Erlikosaurus* (Clark et al., 1994), and dromaeosaurids (Norell and Makovicky, 2004; Norell et al., 2006) differ from the condition in *Zuolong* because in these taxa the quadrate foramen is a tall oval rather than slit-like and developed as an opening between the quadrate and quadratojugal rather than as a foramen within the quadrate.

Pterygoid—The left pterygoid is complete and preserved in articulation with the quadrate posteriorly and the ectopterygoid anteriorly (Fig. 3B). It is tetraradiate, composed of a tall, narrow quadrate ramus, a posteroventromedially directed pterygoid flange, a ventrolaterally directed ectopterygoid ramus, and an anteroposteriorly oriented vomeropalatine ramus. Medially, the quadrate ramus is nearly flat, with a slight medial curve at the ventral border. The junction between the quadrate ramus of the pterygoid and the body of the pterygoid is strongly twisted medially and posteriorly to form a small, posteriorly directed flange. The basipterygoid articular surface on the medial surface of this flange is shallowly concave. The region between the quadrate ramus and the flange houses a deep fossa that opens dorsally. Anterior to the pterygoid flange, the pterygoid body extends anteroventrally as a narrow sheet that contacts the dorsal margin of the ectopterygoid and forms the dorsal margin of the ectopterygoid vacuity. The vomeropalatine ramus extends anterior to the ectopterygoid ramus as a thin bar of bone. A sliver of bone is preserved in contact with the anterior end of the vomeropalatine ramus. The anteroposteriorly long, mediolaterally narrow morphology of this piece of bone suggest that it is the posterior end of the vomer, rather than the pterygoid process of the palatine. The lateral surface of this piece of the vomer is concave, suggesting an articulation with the palatine.

Ectopterygoid—The right ectopterygoid is incomplete, consisting of only the jugal process, and it is separate from other skull bones. The left ectopterygoid is complete and preserved in articulation with the pterygoid (Fig. 3A, C, D). The ectopterygoid consists of a subtriangular body and a thin, tubular, posteriorly curving jugal process. The dorsal, medial, and posterior surfaces of the ectopterygoid body contact the pterygoid. A deep recess extends from the medioventral surface anterodorsally into the ectopterygoid body. A narrow shelf restricts the opening to the recess anteriorly. This recess is more pronounced, and it has thinner walls, than in more basal theropod taxa such as *Allosaurus* (Madsen, 1976), but it is similar to the condition seen in most derived coelurosaurians, particularly *Deinonychus* and other dromaeosaurids (Ostrom, 1969; Rauhut, 2003; Norell and Makovicky, 2004), where it excavates nearly all of the ectopterygoid body and extends at least partially into the jugal process. In cross-section, the jugal process is ovoid, with the major axis oriented dorsoventrally. It is unclear how far the ectopterygoid recess extends into the jugal process.

Squamosal—The right squamosal is missing the distal portions of the parietal process and the quadratojugal process and most of the opisthotic process (Fig. 4A–C). Small broken pieces of the quadratojugal process of the left squamosal are preserved in articulation with the left quadratojugal. The squamosal is composed of a body with a quadrate cotyle on the lateral surface, an anteroventrally directed quadratojugal process, a distally bifurcating postorbital process, and a posteroventrally directed opisthotic process. The ventral surface of the postorbital process is concave. This concavity, which extends onto the anterior surface of the body of the squamosal, ends proximally in a deep, triangular recess. Anteriorly, the postorbital process divides into lateral and medial laminae. The lateral lamina has a shallow groove along its lateral surface marking the contact with the postorbital. Whether the postorbital contact also extended between the medial and lateral laminae cannot be determined. The anterior end of the

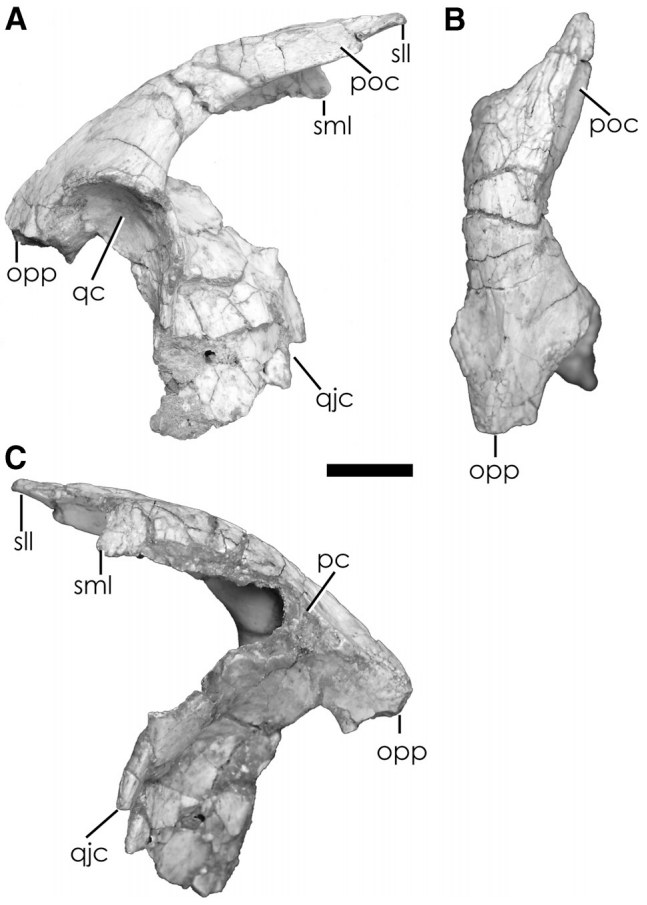

FIGURE 4. Craniodental bones of *Zuolong salleei*. Right squamosal in **A**, lateral view; **B**, dorsal view; **C**, medial view. **Abbreviations**: **opp**, opisthotic process; **pc**, parietal contact; **poc**, postorbital contact; **qc**, quadrate cotyle; **qjc**, quadratojugal contact; **sll**, squamosal lateral lamina; **sml**, squamosal medial lamina. Scale bar equals 3 cm.

medial lamina is broken. The medial surface of the squamosal is broken and the parietal contact is not preserved, but it would have been present along the medial surface of the medial lamina. The quadrate cotyle opens ventrolaterally and the head of the quadrate would have been visible in lateral view. A low, dorsally projecting ridge indicates where the dorsal surface of the squamosal body forms the posterolateral boundary of the supratemporal fenestra. The quadratojugal process has extensive contact with the quadratojugal, and it is parallel to the quadrate. Too little of the opisthotic process is preserved to permit description.

Skull Roof—Most of the frontals and the anterior portion of the parietals are preserved as a single, articulated unit (Fig. 5A–F). The frontoparietal suture has been obliterated by fusion of the two bones. The preserved portions of the frontals are rectangular and longer than wide. The suture between the frontals is visible in dorsal and ventral views. The anterior end of this suture is straight, but the posterior end is complex and interdigitating. Shallow depressions immediately lateral to the interfrontal sutures are developed at the level of the midpoint of the orbit on the dorsal surface. The nasals (which are not preserved) overlapped the frontals, as evidenced by a shallowly depressed, striated region on the anterior end of the dorsal surface of the frontals. There are no notches on the lateral surface of the anterior end of the frontals, indicating that the prefrontal was small. The contact between the frontals and the postorbitals is not preserved. A low ridge of bone defining the anterior margin of the supratemporal fossa extends onto the posterolateral end of the dorsal surface of the frontals. On the ventral surface of the frontals, the cristae cranii are well developed. Shallow depressions that housed the olfactory bulbs lie between the anteriorly diverging portions of the cristae cranii. The cerebral depression located between the posteriorly diverging portions of the cristae crania is wide and triangular, the condition seen in most coelurosaurians (Rauhut, 2003).

The parietals are co-ossified and posteriorly broken. The preserved portion is approximately one-third the length of the frontals. A sagittal crest between the parietals becomes dorsally taller as it extends posteriorly. There is no evidence for a knob-like projection of the posterior-most sagittal crest, as in *Ceratosaurus* (Tykoski and Rowe, 2004), tyrannosaurids (Holtz, 2004), and *Allosaurus* (Madsen, 1976).

Mandible

Angular—The left angular is nearly complete (Fig. 6A–B). It is twisted at its midpoint, producing a 'bow-tie' morphology in lateral view, with the dorsoventrally tall dentary and surangular processes connected at the center by a dorsoventrally short section of cylindrical bone. The mandibular foramen was located immediately dorsal to the dorsoventrally short midsection of the angular, and was relatively large, although not hypertrophied as in oviraptorosaurs (Osmólska et al., 2004). The dentary process, though broken anteriorly, has an articular groove on the ventrolateral surface. The surangular process is narrow, deepening dorsoventrally as it extends posteriorly to its flattened articular surface. The posteromedial surface is concave, and this concavity proceeds anteriorly, becoming dorsally and finally dorsolaterally located. The angular of *Allosaurus* is more mediolaterally flattened and plate-like, whereas the angular of *Tyrannosaurus* tapers sharply anteriorly (Madsen, 1976; Brochu, 2003).

Dentition

We adopt the anatomical conventions proposed by Smith and Dodson (2003) for describing teeth. Three poorly preserved teeth (Fig. 7A–F), including one premaxillary tooth, that range in size from less than 1 to approximately 2 cm in total length were found with the specimen. The best-preserved tooth (Fig. 7A–D) is missing only the ventral root. It has a D-shaped cross-section, with the mesial and distal carinae connected by a planar surface lingually and an anteriorly convex surface labially. This distinctive shape suggests that this is a premaxillary tooth. The labial surface is only moderately convex, unlike the premaxillary teeth of *Guanlong* (IVPP V14531) and *Tyrannosaurus* (Brochu, 2003), where the convexity of the labial surface of the tooth is pronounced and the carinae are only narrowly separated along the lingual edge of the tooth. The premaxillary tooth has small (~6/mm) denticles located on both of its carinae. The denticles are simple and subrectangular, with convex basal and apical edges. The preserved portion of the root is cylindrical, with a constriction between the tooth root and crown on the distal surface. The remaining two teeth are narrow and recurved, morphology consistent with the maxillary and dentary teeth of most theropods. The larger of these maxillary/dentary teeth (Fig. 7E) is 1.9 cm in total length. This tooth is badly broken, and the apex of the crown, the basal end of the root, and most of the distal carina are missing. There is no constriction at the basal portion of the crown. The mesial carina of the crown is smooth, whereas the preserved portion of the distal carina bears small denticles (~6/mm). Damage to both carinae does not permit assessment of the basal extent of either carina. The missing crown portion makes it impossible to rule out the presence of denticles on the mesial carina, but if they were present they were located apically. The basal

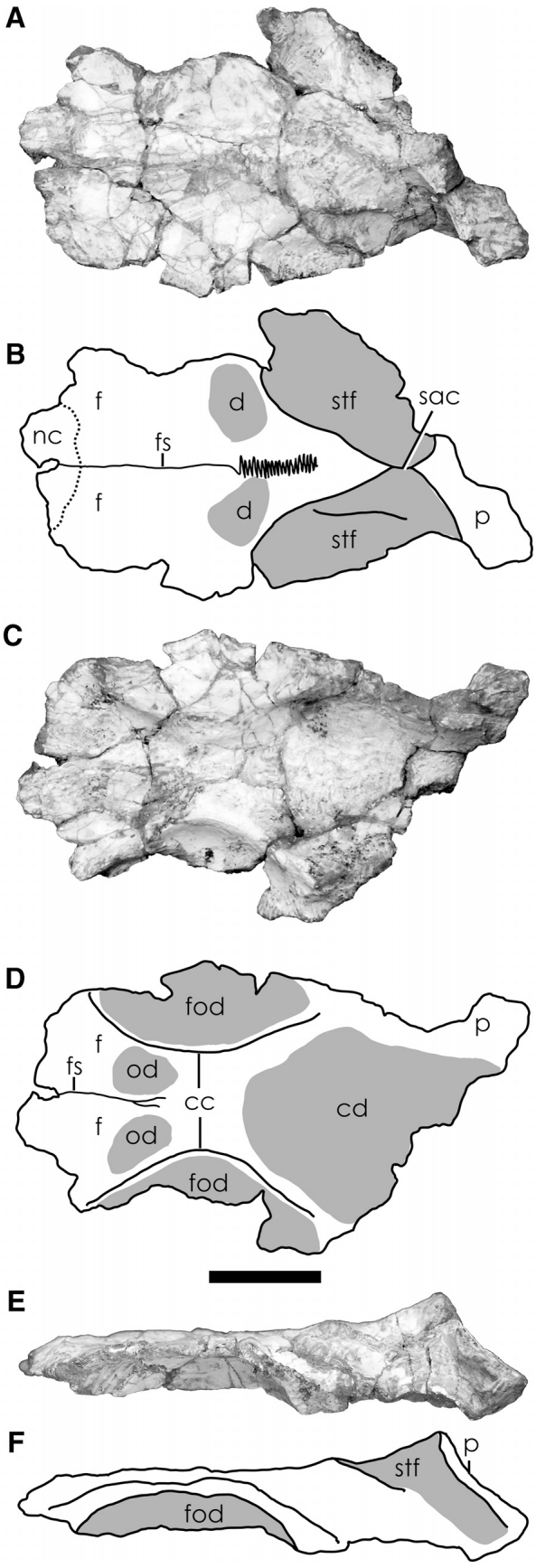

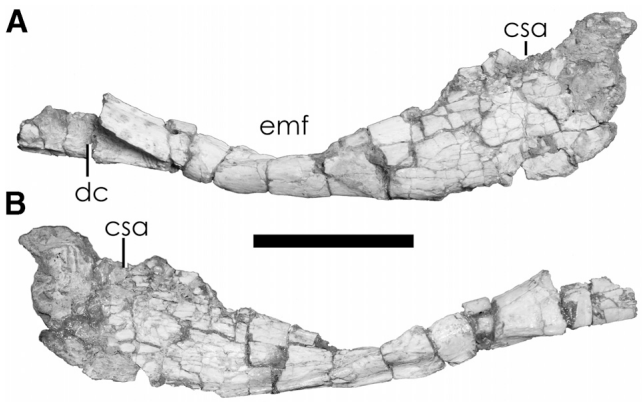

FIGURE 6. Craniodental bones of *Zuolong salleei*. Left angular in lateral view. **Abbreviations**: **csa**, contact with surangular; **dc**, contact with dentary; **emf**, external mandibular fenestra. Scale bar equals 3 cm.

portion of the crown is slightly constricted labiolingually. Distinct, 'band-like' horizontal enamel wrinkles (Brusatte et al., 2007) extend across the entire tooth root and the basal portion of the crown. The morphology of these wrinkles is consistent with those of tyrannosauroids, *Allosaurus*, *Fukuiraptor*, and *Megalosaurus bucklandii* (Smith, 2005; Brusatte et al., 2007), but not with those of carcharodontosaurids (Brusatte et al., 2007). The smaller maxillary/dentary tooth (Fig. 7F) is missing the tip of the crown and the entire root and measures approximately 0.5 cm long as preserved. This tooth bears small denticles (~6/mm) of equal size on its anterior and distal carinae. The denticles are rectangular, with convex basal and apical margins. The distal carina extends to the base of the crown, but the basal portion of the mesial carina is broken and the extent of its denticles cannot be determined.

Axial Skeleton

Without soft-tissue preservation, determining whether the fossae and foramina in the axial column of many theropods (e.g., O'Connor and Claessens, 2005) are pneumatic or nutritive features is problematic. The most robust hypotheses of axial pneumaticity rely on the presence of large internal spaces in the vertebrae, numerous cortical foramina, and deep fossae (O'Connor, 2006). The axial column of *Zuolong* features cortical foramina in some of the centra, but the centra generally lack deep fossae and broken pieces of vertebrae preserved with the skeleton show no evidence of large internal chambers. We therefore cannot strongly hypothesize that the vertebral foramina of *Zuolong* are related to the pulmonary system.

The neurocentral sutures of the cervical vertebrae are easily discerned, and the sutural marks on the dorsal surface of the dorsal centra indicate that the neural arches were not completely fused. These data suggest that the *Zuolong* holotype is the

← FIGURE 5. Craniodental bones of *Zuolong salleei*. Frontal and parietal in **A**, **B**, dorsal view; **C**, **D**, ventral view; **E**, **F**, left lateral view. Shaded grey areas in line drawings **B**, **D**, **F** represent depressions. **Abbreviations**: **cc**, cristae cranii; **cd**, depression for cerebrum; **d**, depression; **f**, frontal; **fod**, orbital depression; **fs**, frontal suture; **nc**, frontal-nasal contact; **od**, depression for olfactory bulbs; **p**, parietal; **sac**, sagittal crest; **stf**, supratemporal fossa. Scale bar equals 3 cm.

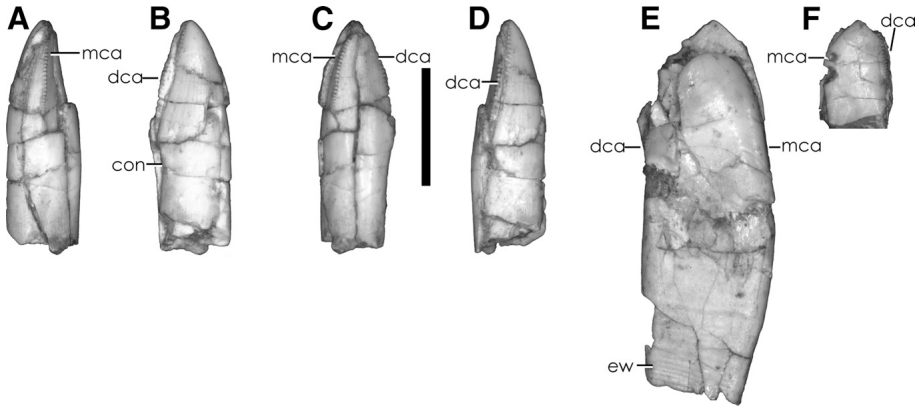

FIGURE 7. Teeth of *Zuolong salleei*. **A**–**D**, Premaxillary tooth in **A**, mesial; **B**, labial; **C**, lingual; **D**, distal views. **E**, **F**, maxillary teeth in labial view. **Abbreviations**: **con**, constriction; **dca**, distal carina; **ew**, enamel wrinkles; **mca**, mesial carina. Scale bar equals 5 mm.

skeleton of an immature individual (Brochu, 1996), although caution should be applied when using neurocentral closure as the sole determinant of developmental stage (Irmis, 2007).

Cervical Vertebrae—Two partial cervical neural arches (C2?, C10?) and five nearly complete cervical vertebrae (C3?–C5?, C8?, C9?) are preserved (Fig. 8A–DD). Although these vertebrae can be confidently assigned to the cervical series, identification of their positions in the series is tentative because their original locations in the block were not recorded. The smaller of the neural arches (Fig. 8A–D) is the shortest cervical vertebra, and it is missing the prezygapophyses and the right central articulation. The neural spine is long and tall, extending beyond the posterior level of the base of the neural arch, and it widens anteriorly and posteriorly. There are well-developed epipophyses overhanging the postzygapophyseal facets. This morphology suggests that the small neural arch belongs to the axis.

The smallest nearly complete cervical vertebra (Fig. 8E–I) is an anterior member of the series, possibly C3. It is missing the articular facets of the prezygapophyses and the left postzygapophysis. The centrum is about twice as long as it is tall, unlike the elongate anterior cervical vertebrae of the basal coelurosaurians *Coelurus* (YPM 2010) and *Guanlong* (IVPP V14531), which are approximately three times longer than they are tall. It has oblique articular surfaces where the dorsal margin is located anterior to the ventral margin in lateral view. The anterior articular surface is wider than high and bears a small depression dorsally for the neural canal. This 'kidney-shaped' morphology with the lateral sides of the anterior articular facet higher than the mesial portion was proposed as a coelurosaurian synapomorphy (Gauthier, 1986; Rauhut, 2003). The posterior articular surface is concave, with a posteriorly projecting ventral lip that extends beyond the posterior level of the dorsal margin. The posteriorly projecting ventral lip is present on the mid-cervical vertebrae of many theropods, including *Monolophosaurus* (Zhao and Currie, 1994), *Allosaurus* (Madsen, 1976), tyrannosauroids (Brochu, 2003; Xu et al., 2006), *Falcarius* (UMNH V12380–12385), *Ornitholestes* (AMNH 619), dromaeosaurids, and troodontids (Makovicky and Norell, 2004; Norell and Makovicky, 2004; Carpenter et al., 2005b). The oblique orientations of the anterior and posterior articular surfaces and the ventral lip are best developed on cervical vertebrae in the region of maximum cervical curvature. The ventral surface of the centrum is smooth and convex. On the anterior end of the ventral surface, small fossae on the ventral surface of the parapophyseal facets extend towards the midline from the lateral margin, creating a short, low, rounded ridge between them.

Recesses are present on the lateral surface of the centrum directly dorsal to the parapophyses, but poor preservation and matrix infill make it impossible to confirm whether they are foramina or deep depressions. The neural canal is large and circular. The neural arch is firmly sutured to the centrum and the contact between the two is almost indistinguishable. The neural arch is as long as the centrum. The neural spine is shorter than the height of the neural arch measured from the central articulation to the dorsal edge of the prezygapophyses and it is centrally located on the vertebra. From the anterior and posterior surfaces of the neural spine, large, triangular interspinous ligament fossae extend onto the dorsal surface of the neural arch. The ventrolaterally oriented transverse process is small and triangular in dorsal view. The posterior centrodiapophyseal lamina buttresses the transverse process. A well-developed, distally incomplete epipophysis on the right postzygapophysis would have extended posteriorly beyond the level of the postzygapophyseal facet.

A mid-cervical vertebra, possibly C4 (Fig. 8J–N), is missing the zygapophyses and the majority of the neural spine. The centrum is long and low, approximately two and a half times as long as it is tall. The lateral surface of this centrum bears shallow depressions dorsal to the parapophyses. The depressions do not contain foramina. The parapophysis is large, approximately two-thirds of the height of the anterior end of the centrum. The anterior articular surface is flat and slightly wider than tall. The posterior articular surface is similar to that of C3? in that it is deeply concave and the ventral margin bears a posteriorly projecting lip. The ventral surface of the centrum is flat and smooth. The neurocentral suture is readily distinguishable. The neural spine is approximately half as long as the centrum, and sits posteriorly on the neural arch.

The longest cervical vertebra is probably C5 (Fig. 8O–S). It is missing the left prezygapophysis, the right postzygapophysis, and the neural spine. Like C3? and C4?, the ventral surface of the centrum and the articular surfaces are oriented obliquely. A deep foramen is located immediately dorsal to the parapophysis, and a shallow, horizontal fossa on the lateral surface of the centrum is continuous with this foramen. In *Guanlong* (IVPP V14531), the foramen in the lateral surface of the centrum of C4 is larger and the horizontal fossa is deeper. The parapophyses of *Zuolong* are approximately half the height of the anterior end of the centrum. The anterior articular surface is slightly convex and as tall as it is wide. The posterior surface is deeply concave and bears a posteriorly projecting lip on the ventral margin. The ventral surface is flat and smooth, except for a small, shallow fossa between the parapophyses. The suture between the neural

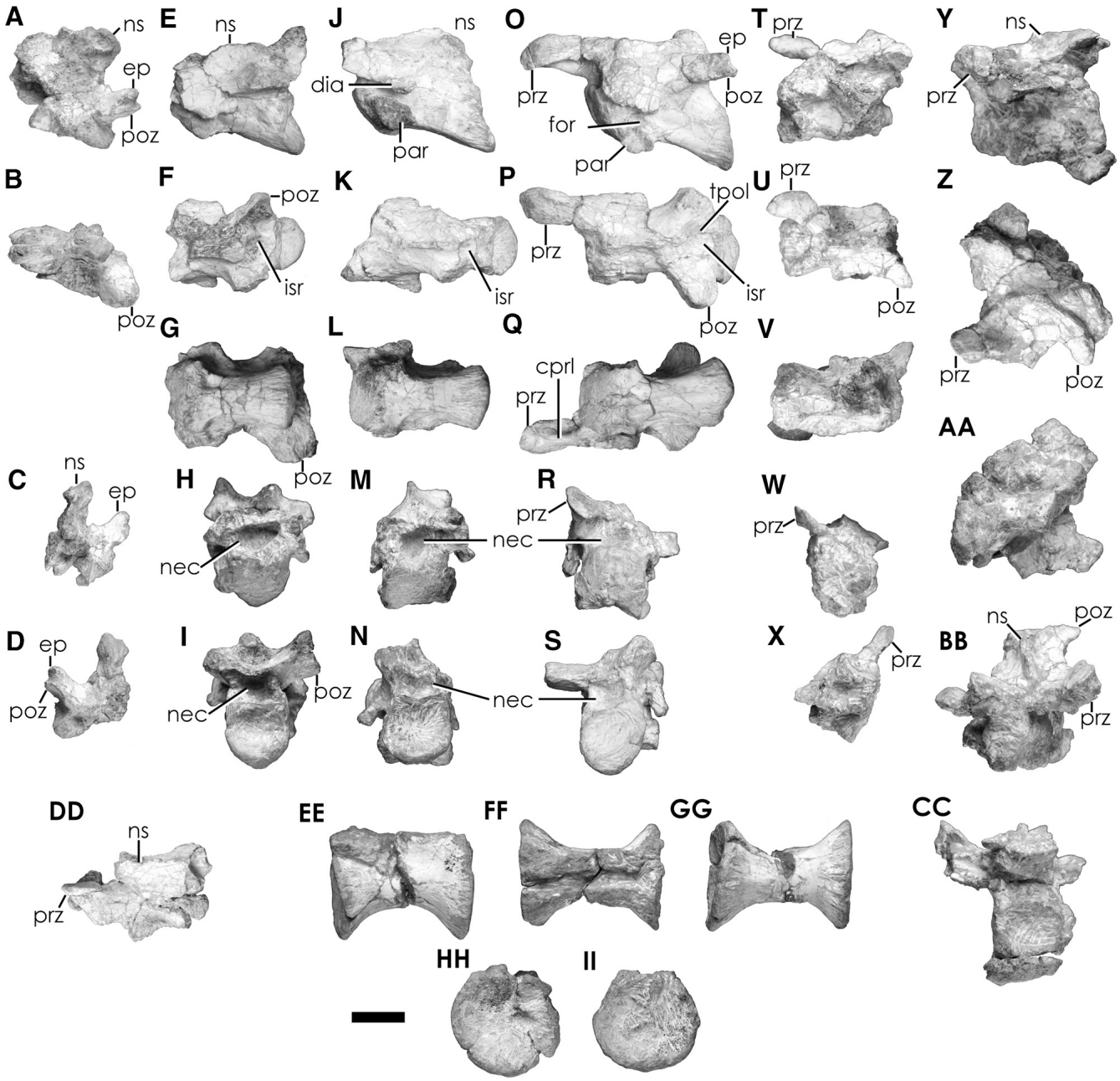

FIGURE 8. Cervical vertebrae of *Zuolong salleei*. **A–D**, ?axial neural arch in **A**, left lateral; **B**, dorsal; **C**, anterior; **D**, posterior views. **E–I**, anterior cervical vertebra (C3?) in **E**, left lateral; **F**, dorsal; **G**, ventral; **H**, anterior; **I**, posterior views. **J–N**, mid-cervical vertebra (C4?) in **J**, left lateral; **K**, dorsal; **L**, ventral; **M**, anterior; **N**, posterior views. **O–S**, mid-cervical vertebra (C5?) in **O**, left lateral; **P**, dorsal; **Q**, ventral; **R**, anterior; **S**, posterior views. **T–X**, posterior cervical vertebra (C8?) in **T**, left lateral; **U**, dorsal; **V**, ventral; **W**, anterior; **X**, posterior views. **Y–CC**, posterior cervical vertebra (C9?) in **Y**, left lateral; **Z**, dorsal; **AA**, ventral; **BB**, anterior; **CC**, posterior views. **DD**, posterior cervical neural arch (C10?) in dorsal view. **EE–II**, representative dorsal centrum in **EE**, lateral; **FF**, dorsal; **GG**, ventral; **HH**, anterior; **II**, posterior views. **Abbreviations**: **cprl**, centroprezygapophyseal lamina; **dia**, diapophysis; **ep**, epipophysis; **for**, foramen; **isr**, interspinous ligament recess; **nec**, neural canal; **ns**, neural spine; **par**, parapophysis; **poz**, postzygapophysis; **prz**, prezygapophysis; **tpol**, intrapostzygapophyseal lamina. Scale bar equals 3 cm.

arch and the centrum is clearly visible in lateral view. The neural arch is longer than wide. The prezygapophysis projects anteriorly and slightly laterally and the prezygapophyseal facets are flat, whereas in many coelurosaurians the prezygapophyses are flexed and the facets are convex (Gauthier, 1986; Rauhut, 2003). The medial surfaces of the bases of the centroprezygapophyseal lamina bear deep fossae adjacent to the neural canal. The postzygapophyses are directed almost completely laterally and they bear well-developed epipophyses that extend to the level of the posterior margin of the postzygapophyseal articular surfaces. The postzygapophyses are connected medially by an intrapostzygapophyseal lamina (Wilson, 1999) that extends posteriorly to the level of the posterior margin of the zygapophyseal facets. The neural spine is broken dorsally, but the preserved portion is anteroposteriorly long and centrally located on the vertebra.

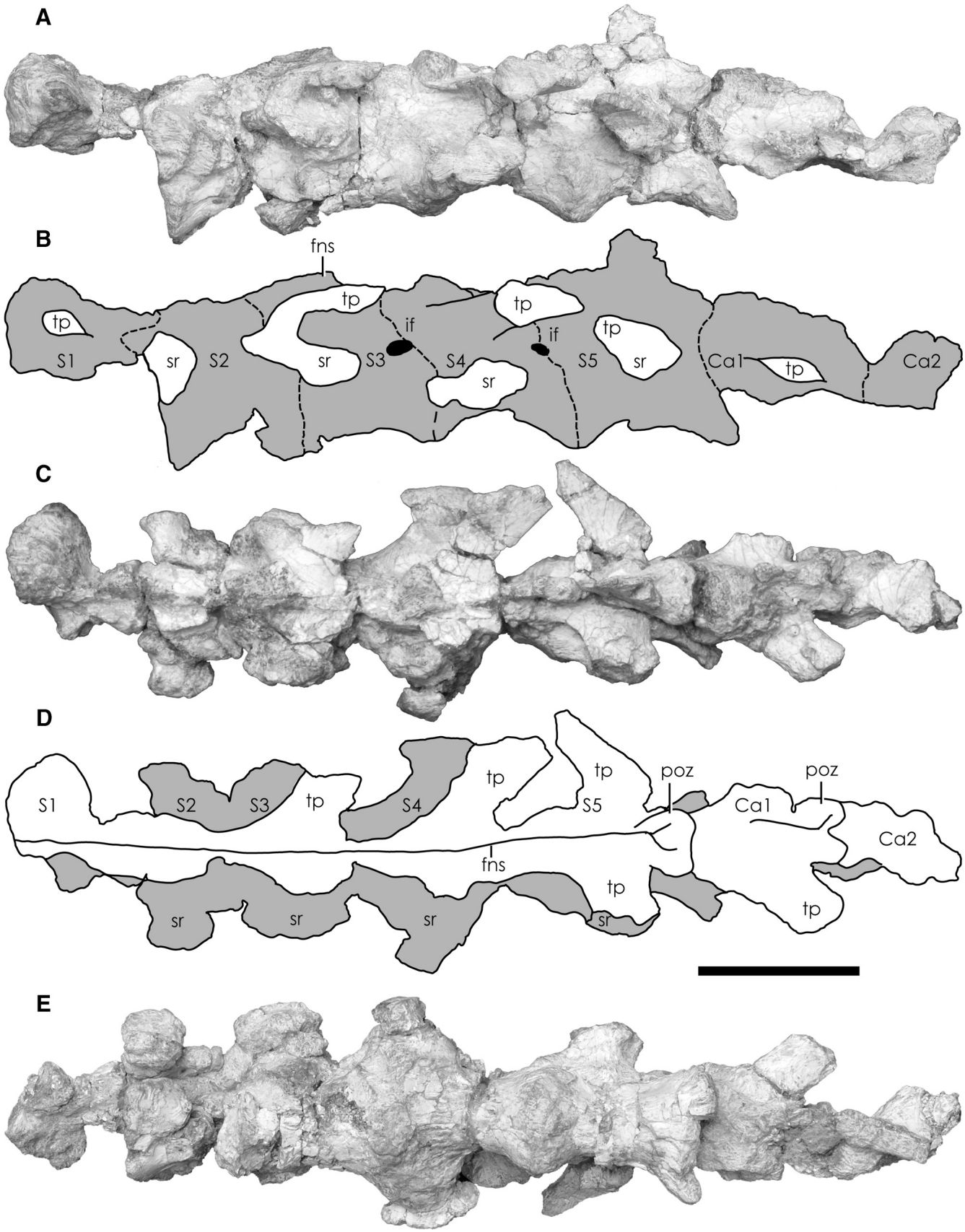

FIGURE 9. Sacrum of *Zuolong salleei*. **A**, **B**, right lateral view; **C**, **D**, dorsal view; **E**, ventral view. **Abbreviations**: **Ca1**–**Ca2**, caudal neural arches; **fns**, fused neural spine; **if**, intervertebral foramen; **poz**, postzygapophysis; **S1**–**S5**, sacral centra; **sr**, sacral rib; **tp**, transverse process. Scale bar equals 5 cm.

Two nearly complete posterior cervical vertebrae probably are C8 and C9. These vertebrae are encrusted by an extremely tough black substance and cannot be fully prepared from the matrix. The smaller of these vertebrae (Fig. 8T–X) is missing the posterior articular surface of the centrum, the neural spine, the left prezygapophysis, and the postzygapophyses. The centrum is less than twice as long as it is tall, and the concave anterior articular surface is oriented at a right angle to the ventral surface. A small foramen is present on the lateral surface dorsal to the parapophysis. The ventral surface is flat. Matrix still covers the area of the suture between the neural arch and the centrum, so neurocentral fusion in this vertebra cannot be determined. The neural arch is slightly longer than wide. The prezygapophysis is short and the articular surface is oriented at a 45° angle to horizontal. The base of the neural spine is about half the length of the centrum and it is located posteriorly on the vertebra. The larger of the two posterior cervical vertebrae (Fig. 8Y–CC) is missing the anterior articular surface of the centrum and the neural spine. Although longer than the other posterior cervical vertebra, it is still shorter than the mid-cervical vertebrae. The lateral surface is obscured by matrix. The posterior articular surface is shallowly concave and much wider than tall. The ventral surface is convex. The neural arch is approximately as long as wide. The prezygapophyses project anterolaterally and their articular surfaces are oriented 45° to the horizontal. The ventral surfaces of the prezygapophyses are buttressed by a poorly preserved prezygadiapophyseal lamina (Wilson, 1999). The transverse processes are poorly preserved and laterally broken, but are supported by anterior and posterior centrodiapophyseal laminae (Wilson, 1999). The postzygapophyses are small and do not bear epipophyses. The short neural spine occupies only the middle one-third of the neural arch.

The larger of the two neural arches (Fig. 8DD) is broken along an anteroposterior line running parallel to the neural spine and it is missing almost the entire right side and the left postzygapophysis. It is as long as wide and it has widely separated prezygapophyses with articular surfaces oriented almost vertically. Based on the relative sizes of the posterior cervical vertebrae, this neural arch may belong to C10. The neural spine of this arch spans the dorsal surface between the pre- and postzygapophyses.

Dorsal Vertebrae—Two complete and two fragmentary dorsal centra are preserved (representative dorsal centrum shown in Fig. 8EE–GG). No neural arches are preserved for the dorsal vertebrae. The two complete dorsal centra are amphicoelous, spool-shaped, and lack fossae and foramina on their lateral surfaces. The ventral surfaces of these centra are smooth and convex.

Sacrum—The sacrum (Fig. 9A–E) is badly broken and partially covered by an extremely hard, black matrix. From anterior to posterior, it consists of a neural arch, four complete sacrals, and two caudal neural arches. The anterior neural arch is well fused to, and bears a continuous neural spine with, the four successive neural arches. The posterior two neural arches have posterolaterally projecting transverse processes, unfused zygapophyses, and separate neural spines, morphologies consistent with caudal vertebrae. We therefore propose that *Zuolong* had five sacral vertebrae, like most basal coelurosaurians (Rauhut, 2003), that the anterior neural arch is sacral vertebra 1 (S1), that the four complete vertebrae are S2–S5, and that the two posterior neural arches are the anterior two caudal vertebrae (Ca1–Ca2). Sacral centra S2–S5 are spool-shaped and fused together at the intercentral articulations. The lateral surfaces of the centra are poorly preserved, but show no fossae or foramina in the preserved regions. The ventral surfaces of the centra are convex, and they do not bear axial sulci. The anterior articular surface of centrum S2 is flat and much wider than tall. The posterior articular surface of S3 and the anterior articular surface of S4 are mediolaterally enlarged, forming an intercentral junction between S3 and S4 that is mediolaterally wider than any other preserved intercentral junction. The posterior articular surface of centrum S5 is concave, wider than tall, and anterodorsally inclined at approximately 60° relative to the horizontal plane of the ventral surface of the synsacrum. This morphology has not been previously reported in a theropod. The preservation of undistorted postzygapophyses and neural spine above this surface indicate that the inclination of the posterior sacral articular surface is not an artifact of deformation.

The zygapophyses of S1–S5 are fused. There are two small intervertebral foramina between the anteroventral margins of the prezygapophyses and the posteroventral margins of the postzygapophyses of S2/S3 and S3/S4. The prezygapophyses strongly overlap the dorsal surfaces of the preceding sacral centra. The postzygapophyses of S5 are separated medially by an interspinous ligament fossa and they are unfused to the prezygapophyses of Ca1. The sacral neural spines are all dorsally broken. From the continuity of their bases, they probably formed one continuous ridge along the length of the sacrum. The neural arch of S1 is too poorly preserved to describe. The transverse processes of S2 are broken proximally. The sacral ribs of S2 are mediolaterally narrow and were not fused to the transverse processes. The laterally broken transverse process of S3 projects posterolaterally. The anterior end of the ventral surface of the transverse process of S3 is fused to the dorsal surface of the laterally projecting sacral rib. In lateral view, this fusion creates a U-shaped contact with the ilium, with the opening of the U facing posteriorly. A similar pattern of fusion between transverse processes and sacral ribs is seen on S4, but on this vertebra the anterior surface of the transverse process and sacral rib also form an anteriorly concave pocket. The right transverse process of S5 is preserved in an unnatural, anterolateral orientation, and the accompanying sacral rib is not preserved. The left transverse process is in the correct posterolateral orientation and it is fused to the sacral rib along the ventral surface. The anterior surface of these fused bones is anteriorly concave in lateral view, forming the posterior rim of the pocket between the neural arches and ribs of S4 and S5.

Caudal Vertebrae—Eight caudal vertebrae are preserved, including one anterior caudal centrum (Fig. 10A–E), one nearly complete anterior caudal vertebra (Fig. 10F–J), two mid-caudal centra (Fig. 10K–T), three nearly complete mid-caudal vertebrae (Fig. 10U–II), and one mid-caudal neural arch (Fig. 10JJ–MM). An anterior position (Ca4?) is likely for the relatively complete caudal vertebra because it bears a centrally placed neural spine, anteroposteriorly long, mediolaterally wide, and centrally placed transverse processes, and postzygapophyses that extend from the neural arch instead of the neural spine and that are at the same level as the transverse processes. The complete centrum referred to as an anterior caudal is slightly larger than the more complete anterior caudal centrum, but it is almost identical in shape and therefore probably lies more anterior in the caudal series. The centra of the remaining six caudal vertebrae become sequentially longer and lower and, where preserved, the neural spines are posteriorly inclined and posteriorly located. The transverse processes of these vertebrae, where preserved, are posteriorly located. The postzygapophyses lie on the posterolateral surfaces of the neural spines. These morphologies indicate mid-caudal positions, and the close matches in size between the anterior and posterior articular surfaces suggest that these six vertebrae form a consecutive series.

The anterior caudal centra do not bear fossae or foramina on their lateral surfaces. The concave anterior articular surfaces are circular and greater in diameter than the flat, box-like posterior articular surfaces. The ventral surfaces are smooth and convex, although the anterior end of the ventral surface of the smaller anterior caudal centrum bears a very shallow groove. The sutural line between the neural arch and centrum of the smaller anterior caudal is easily discerned. The prezygapophyses nearly touch each other above the neural canal, extend a short distance

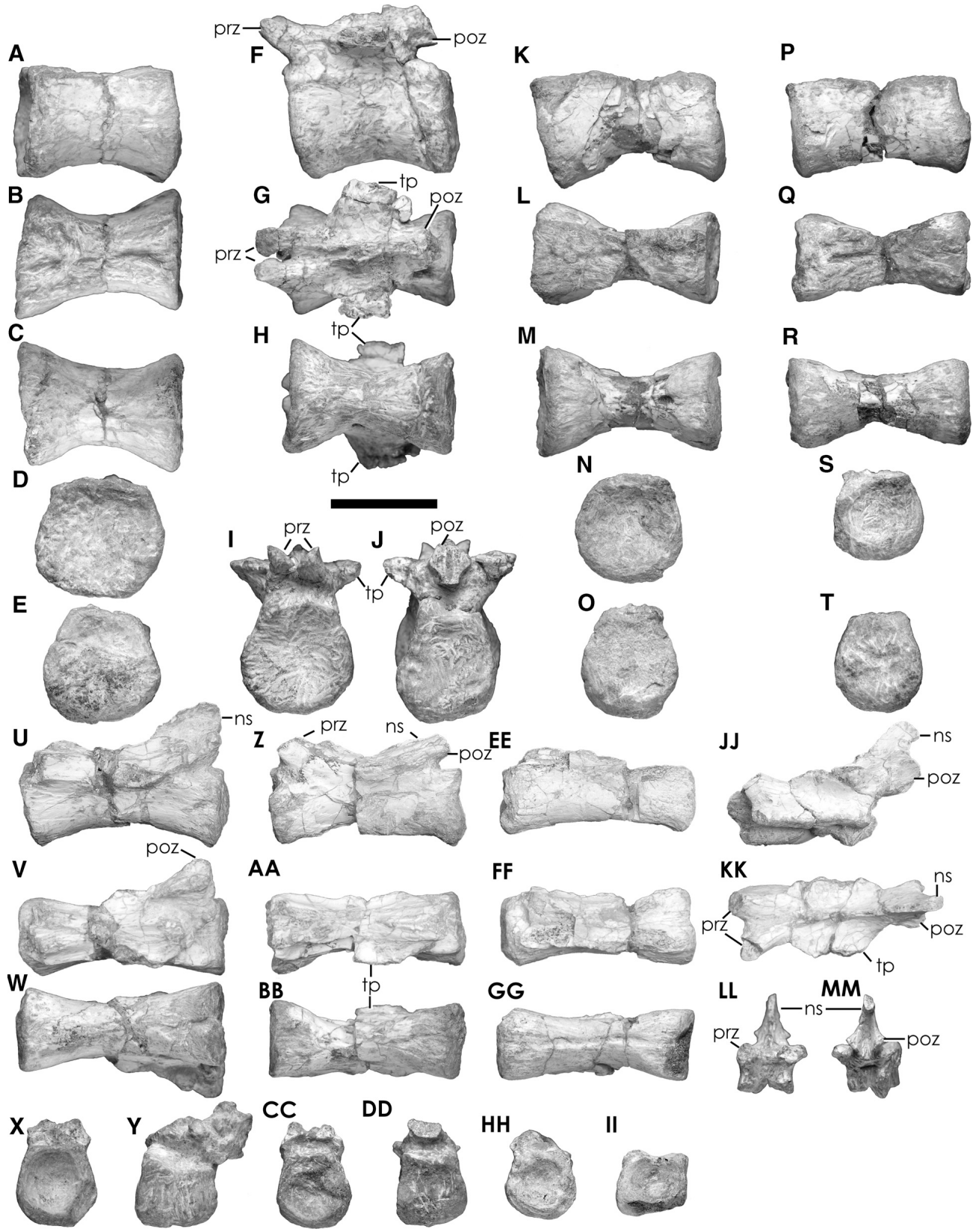

FIGURE 10. Caudal vertebrae of *Zuolong salleei*. **A**–**E**, anterior caudal vertebra (Ca3?) in **A**, lateral; **B**, dorsal; **C**, ventral; **D**, anterior; **E**, posterior views. **F**–**J**, anterior caudal vertebra (Ca4?) in **F**, lateral; **G**, dorsal; **H**, ventral; **I**, anterior; **J**, posterior views. **K**–**O**, mid-caudal vertebra in **K**, lateral; **L**, dorsal; **M**, ventral; **N**, anterior; **O**, posterior views. **P**–**T**, mid-caudal vertebra in **P**, lateral; **Q**, dorsal; **R**, ventral; **S**, anterior; **T**, posterior views. **U**–**Y**, mid-caudal vertebra in **U**, lateral; **V**, dorsal; **W**, ventral; **X**, anterior; **Y**, posterior views. **Z**–**DD**, mid-caudal vertebra in **Z**, lateral; **AA**, dorsal; **BB**, ventral; **CC**, anterior; **DD**, posterior views. **EE**–**II**, mid-caudal vertebra in **EE**, lateral; **FF**, dorsal; **GG**, ventral; **HH**, anterior; **II**, posterior views. **JJ**–**MM**, mid-caudal vertebra in **JJ**, lateral; **KK**, dorsal; **LL**, anterior; **MM**, posterior views. **Abbreviations**: **cns**, suture between centrum and neural spine; **ns**, neural spine; **poz**, postzygapophysis; **prz**, prezygapophysis; **tp**, transverse process. Scale bar equals 3 cm.

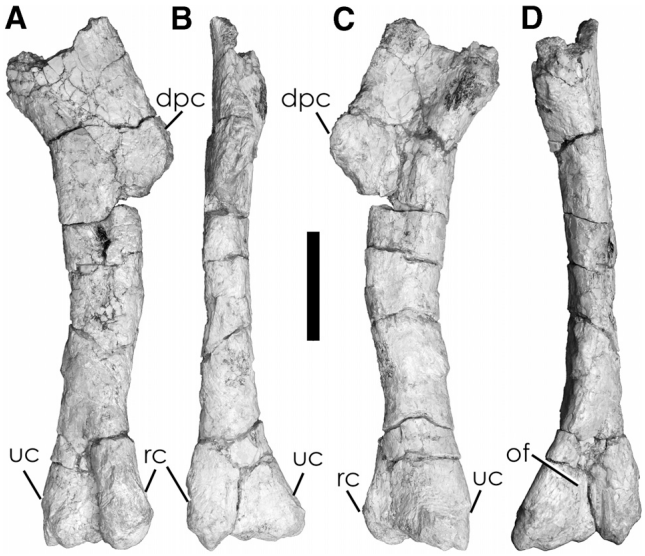

FIGURE 11. Right humerus of *Zuolong salleei*. **A**, lateral; **B**, anterior; **C**, medial; **D**, posterior views. **Abbreviations: dpc**, deltopectoral crest; **of**, olecranon fossa; **rc**, radial condyle; **uc**, ulnar condyle. Scale bar equals 3 cm.

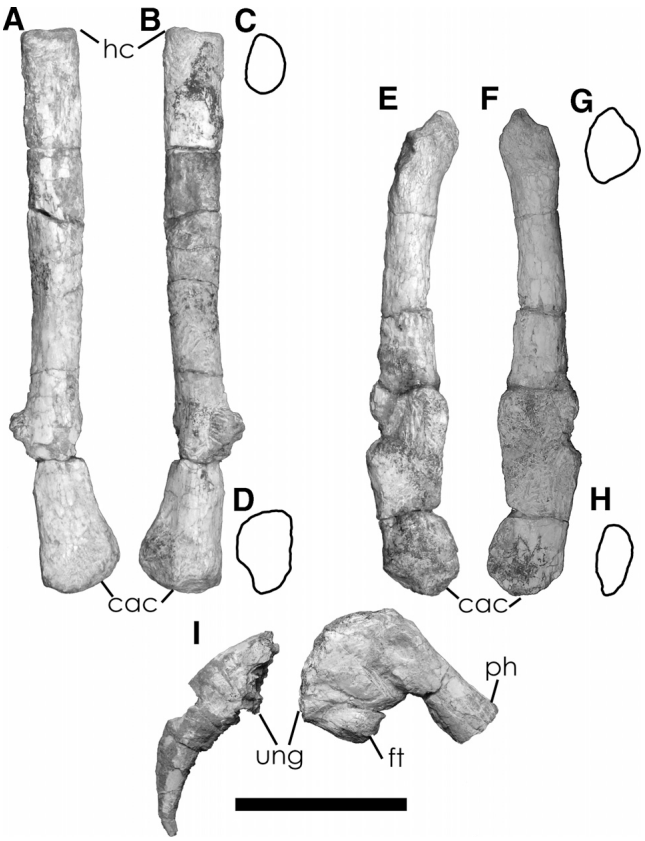

FIGURE 12. Left radius, ulna, and manual bones *Zuolong salleei*. Left radius in **A**, lateral view; **B**, medial view; **C**, proximal outline; **D**, distal outline. Left ulna in **E**, medial view; **F**, lateral view; **G**, proximal outline; **H**, distal outline. **I**, distal manual phalanx and ungual. **Abbreviations**: **cac**, carpal contact; **ft**, flexor tubercle; **hc**, humeral contact; **ph**, phalanx; **ung**, ungual. Scale bar equals 3 cm.

past the anterior margin of the centrum, and have dorsomedially oriented articular surfaces. The transverse processes are laterally broken, but their bases are long. The postzygapophyses are broken posteriorly, and, as preserved, extend only to the dorsal rim of the centrum. The postzygapophyseal bases are close together, which would have placed the postzygapophyseal facets next to one another above the neural canal.

The six mid-caudal vertebrae do not bear fossae or foramina on their lateral surfaces. The centra become successively longer from the anterior-most centrum of this series, which is twice as long as tall, to the elongated posterior centrum, which is three times as long as tall. The centra have concave anterior and flat posterior articular surfaces; only the posterior-most centrum has biconcave articular surfaces. The ventral surface of each mid-caudal centrum is concave and has a shallow axial groove. The four preserved mid-caudal neural arches all lack the anterior ends of the prezygapophyses. The postzygapophyses are best preserved on the isolated neural arch. These sit on the posteroventral margin of the neural spine, extend beyond the posterior level of the neural arch, face ventrolaterally, and are located on a level above the plane of the transverse process. The neural spine of this vertebra is strongly inclined posteriorly. The neural spine lacks an anterior 'spur' or ala, unlike the neural spines of the mid-caudals of *Allosaurus*, carcharodontosaurids, *Sinraptor*, *Afrovenator*, and *Siamotyrannus* (Rauhut, 2003). The preserved portion of the tall, slender neural spine extends posterodorsally.

Pectoral Girdle and Forelimb

Scapula—The bones of the pectoral girdle consist only of a poorly preserved right scapula (not figured). The blade of the scapula is long and narrow, at least nine times as long as it is wide. The distal end is incomplete, but appears to be only slightly expanded. The proximal end is not well enough preserved to assess the extent of the acromion process or the morphology of the glenoid.

Humerus—A nearly complete right humerus (Fig. 11A–D) is preserved. It is missing the head, the posteroproximal portion of the internal tuberosity, the anteroproximal surface of the deltopectoral crest, and the distal ends of the distal condyles. The humerus is approximately 46% the length of the femur. The distal end of the quadrangular deltopectoral crest projects from the proximal one-third of the humeral shaft at an approximate 45° angle from the anterior margin. The expanded distal end of the right humerus has a well-developed olecranon fossa on the posterior surface. The distal-most ends of both the radial and the ulnar condyles are eroded, but the preserved portions are subequal in size. Epicondyles are not preserved.

Radius—The left radius is nearly complete (Fig. 12A–D).The straight and slender bone is 88% the length of the humerus, a ratio consistent with most theropods other than tyrannosauroids, baryonychids, abelisaurids, and *Torvosaurus* (Rauhut, 2003). The proximal end is ovoid in proximal view. The distal end of the radius is convex, roughly triangular in distal view and bears a small ventral expansion that is common to many theropods. The medial surface is flat for articulation with the distal end of the ulna.

Ulna—The slender left ulna (Fig. 12E–H) is only slightly curved and similar in diameter to the radius. The proximal end is missing approximately 2 cm of the shaft, including the olecranon process and the humeral articular facet. The ulnar shaft is broken close to the midpoint; distal to this break, the shaft is mediolaterally flattened. It is unclear whether this flattening is due to diagenetic deformation. The distal articular surface of the ulna is badly eroded, but the preserved portion shows that it was narrow and tall.

Manus—Preserved manual bones of *Zuolong* are limited to a nearly complete manual ungual preserved in articulation with the distal end of a manual phalanx (Fig. 12I). The distal end of the phalanx has a shallow groove dorsally between the articular condyles. The articular condyles are equal in size and ovoid in lateral view. The collateral ligament fossae are located above the midline of the phalanx. This morphology is consistent with the distal end of the first phalanx of the medial digit of other theropods, but poor preservation and the incompleteness of the bone make this identification tentative. The proximal portion of the manual ungual is narrow, with a well-developed, proximally located flexor tubercle. The proximal end of the dorsal surface lacks the dorsally projecting lip that is sometimes present in derived coelurosaurians (Rauhut, 2003). The manual ungual is strongly curved and the lateral grooves are symmetrically positioned.

Pelvic Girdle and Hind Limb

Ilium—The left ilium is incomplete and preserved in three separate parts: the dorsal iliac rim, the postacetabular ala including the complete ischial peduncle and the posterior half of the iliac acetabulum, and the pubic peduncle including the anterior half of the iliac acetabulum (Fig. 13A–D). The dorsal rim of the ilium is dorsally convex in lateral view, suggesting that the ilium was dorsoventrally tall, and it differs from the dorsally flat, low ilia of many basal tetanurans and some paravians (Ostrom, 1969; Rauhut, 2003; Makovicky and Norell, 2004). It is impossible to tell from the preserved portion of the dorsal rim whether the ilium was inclined toward the sacral neural spines. The postacetabular ala of the ilium is missing the medial portion of the posterior end of the brevis shelf, which is preserved only as a rugose ridge on the medial surface of the postacetabular ala. The posterior end of the postacetabular ala is convex. On the medial surface of the postacetabular process, the brevis shelf begins on the ischial peduncle and extends posterodorsally to the posterior border of the process. The anterior end of the brevis fossa is mediolaterally narrow; the posterior portion of the brevis fossa is also likely to have been narrow because the lateral surface of the postacetabular ala lacks the lateral expansion present in ornithomimosaurs (Rauhut, 2003; Makovicky et al., 2004a) and *Syntarsus* (Raath, 1977). The postacetabular ala diverges laterally at a low angle from the plane of the vertebral column. A supraacetabular crest extends laterally from the anterior half of the acetabulum. Well-developed supraacetabular crests are present in most basal theropods (e.g., *Cryolophosaurus* [Smith et al., 2007], *Syntarsus* [Raath, 1977]), in some basal coelurosaurians (e.g., *Stokesosaurus* [Benson, 2008a], ornithomimosaurs [Makovicky et al., 2004b]), but they are reduced or absent in derived coelurosaurians (e.g., oviraptorosaurs [Osmólska et al., 2004], dromaeosaurids [Norell and Makovicky, 2004]). Posterior to the supraacetabular crest, the acetabulum is laterally broken, and the preserved portions of the ilium do not include the contact between the anterior and posterior halves of the acetabulum. There is no indication of an antitrochanter, a feature characteristic of relatively derived coelurosaurians (e.g., therizinosauroids [Clark et al., 2004], oviraptorosaurs [Osmólska et al., 2004]). The anterior end of the pubic peduncle is broken, and a portion of the articular surface is missing. The pubic peduncle faces anteroventrally. The preserved articular surface of the pubic peduncle is anteroposteriorly longer than it is wide, as in all coelurosaurians (Rauhut, 2003), and mediolaterally wider at the posterior margin where it meets the acetabulum. The posteroventrally oriented ischial peduncle has been eroded distally, but it appears to have a sharp distal edge, as in most other coelurosaurians (Rauhut, 2003) and in *Allosaurus* (Madsen, 1976), which is unlike the broad ischial peduncle of basal tetanurans (Rauhut, 2003).

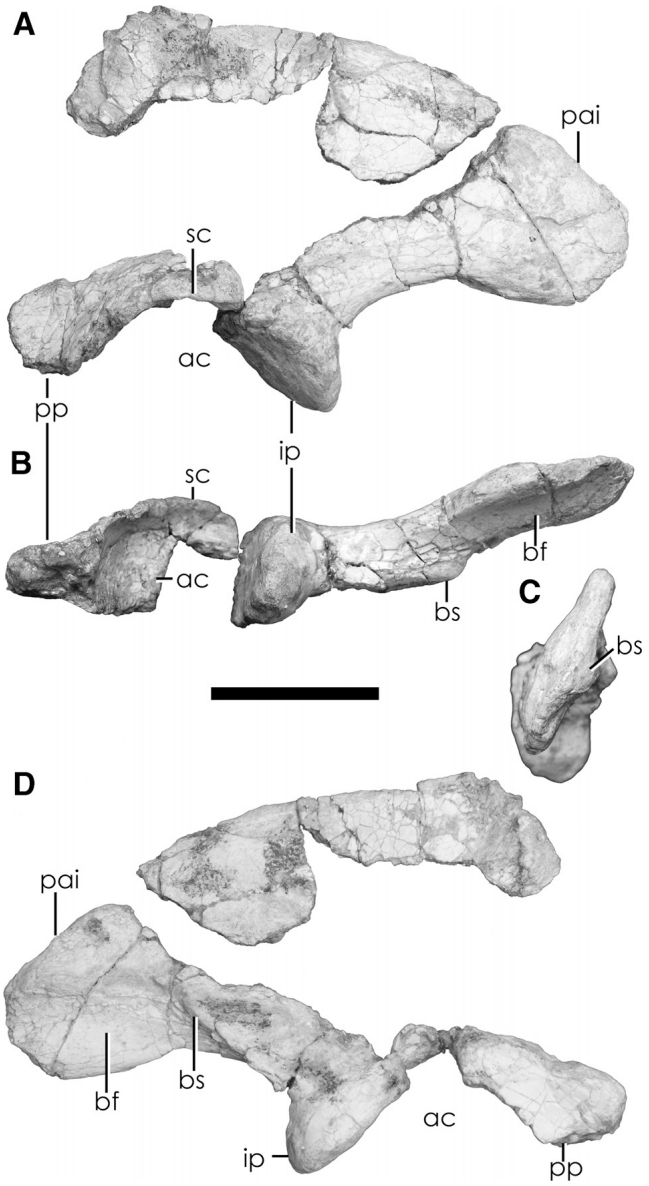

FIGURE 13. Left ilium of *Zuolong salleei*. **A**, lateral; **B**, ventral; **C**, posterior; **D**, medial views. **Abbreviations**: **ac**, acetabulum; **bf**, brevis fossa; **bs**, brevis shelf; **ip**, ischial peduncle; **pai**, postacetabular ala of ilium; **pp**, pubic peduncle; **sc**, supraacetabular crest. Scale bar equals 5 cm.

Pubis—The articulated pubes (Fig. 14A–E) are nearly complete, missing only the proximal left articular surface with the ilium and the anterior and posterior surfaces of the pubic boot. The pubis probably projected anteroventrally, as in most nonparavian theropods, based on the angle of the facet on the iliac pubic peduncle. The puboiliac articular surface is divided into two parts: a subrectangular anterior portion that is twice as long as wide and that would have articulated with the pubic peduncle of the ilium, and a posteriorly tapering, triangular posterior section that is widest at the midpoint of the puboiliac surface, and that constitutes the pubic contribution to the acetabulum. The shape of the rectangular, anterior portion matches the shape of the preserved pubic peduncle of the ilium, and the mediolateral expansion of the posterior portion at the midpoint of the puboiliac surface of the pubis matches the posterior expansion of

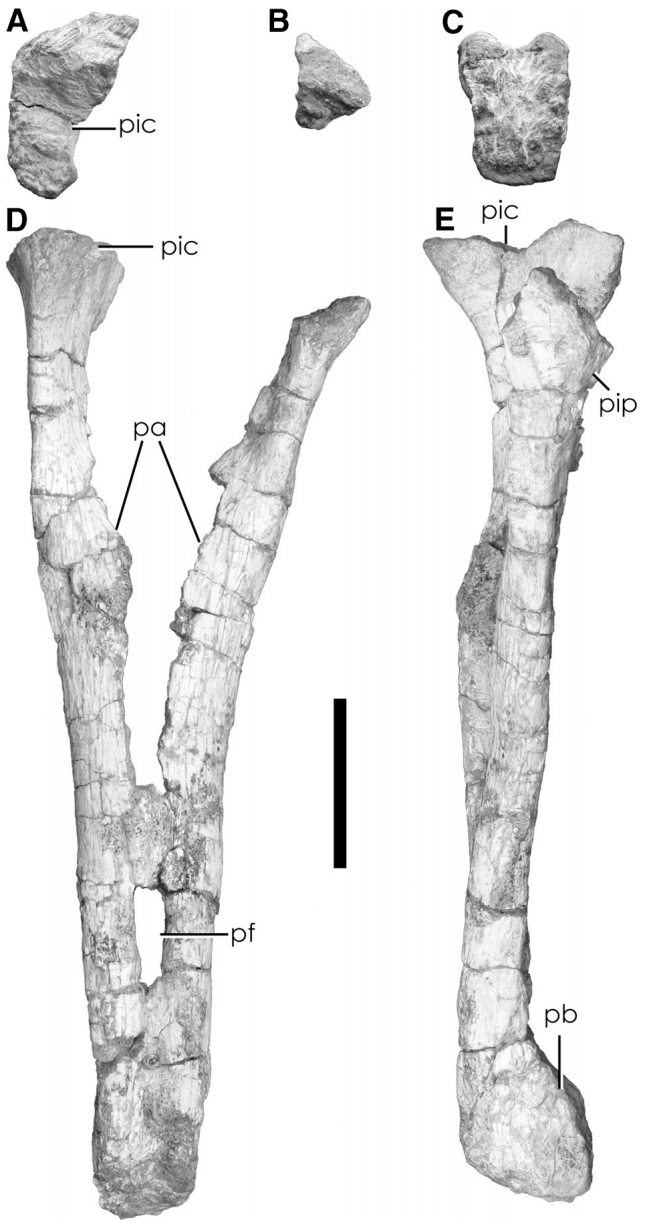

FIGURE 14. Pubes of *Zuolong salleei*. **A**, **B**, proximal; **C**, distal; **D**, anterior; **E**, left lateral views. **Abbreviations: pa**, pubic apron; **pb**, pubic boot; **pf**, pubic foramen; **pic**, puboiliac contact; **pip**, puboischiac plate. Scale bar equals 5 cm.

the iliac pubic peduncle at the anterior margin of the acetabulum. The anterior portion of the proximal surface of the puboiliac articulation bears a depression posteriorly that is deepest medially and ends just medial to the lateral edge. This depression is probably the posterior extent of the iliac pubic peduncle. The posterior portion of the proximal surface has a shallow depression on its posterior margin that marks the pubic contribution to the floor of the acetabulum.

On the posterior surface of the proximal pubic shafts, the base of the puboischiac plate extends only a short distance distally. Due to posterior breakage of this plate, the morphology of the obturator region cannot be determined, but because the plate is low and there is no suggestion of an opening for an obturator foramen preserved on the base, it is likely that the obturator opening was developed as a notch. The puboischiac plate would not have been large enough to bear a pubic foramen. The pubic apron extends proximally up the rod-like pubes as a shelf along the anterior surface. The apron turns posteriorly and extends as a medial ridge that approaches, but does not reach, the articular head of the pubis. Proximal to the pubic boot, an area of matrix infill between the pubic shafts suggests a small 'pubic fenestra,' but poor preservation makes this uncertain. The distal end of the pubis is extensively eroded, making it difficult to determine the full extent of the pubic boot. Based on the lack of anterior expansion of the distal pubic shafts, there was probably little anterior projection of the pubic boot.

Femur—The left femur is complete (Fig. 15A–H), and the preserved distal half of the right femur is badly weathered. The hemispherical head of the femur projects at an approximate 90° angle to the plane of the shaft. Relative to the plane of the distal condyles, the femoral head is oriented approximately 15° anteromedially. This contrasts with the condition in derived coelurosaurians, in which the femoral head is oriented strictly medially (Holtz, 1994; Rauhut, 2003). The Early Cretaceous taxon *Tugulusaurus*, considered a basal coelurosaur by Rauhut and Xu (2005), also has an anteromedially directed femoral head. In *Zuolong*, the head of the femur is confluent with the greater trochanter. A well-developed ligament pit (the fovea capitis) occupies almost the entire posterodorsal corner of the medial surface of the femoral head. It is continuous with an oblique ligament groove on the dorsal portion of the posterior surface of the femoral head, extending laterally as a deep slot that reaches the posteromedial edge of the greater trochanter. In extant avians, the fovea capitis is the osteological correlate of the ligamentum capitis femoris (Duff, 1988), and the presence of the fovea in extinct avians (Mayr et al., 2002) and in some non-avian theropods suggests homology of this feature in these taxa. An extremely large fovea capitis is known from the pathological femoral heads of male turkeys (Duff, 1988), although there is an associated change in contour and texture of the femoral head, neither of which is present in *Zuolong*. Still, pathology cannot be ruled out without the discovery of the contralateral femoral head, and we tentatively propose the enlarged fovea capitis as an autapomorphy for *Zuolong*.

The greater and lesser trochanters are well developed and separate from each other. In proximal view, the greater trochanter is anteroposteriorly longest near the femoral head, and it shortens in this dimension laterally. The alariform lesser trochanter is broken close to its base, but the preserved portion includes the ventral margin of what would have been a deep slot separating it from the greater trochanter. A nutrient foramen at the base of the lesser trochanter is absent, but this may be due to poor preservation. The fourth trochanter is a well-developed, 3-cm-long ridge that is located on the posterolateral surface of the femoral shaft. The fourth trochanter of *Zuolong* is more proximal in position than in ceratosaurs and non-coelurosaurian tetanurans (Rauhut, 2003). The femoral shaft is posteriorly concave. An anterior intermuscular line (Brochu, 2003) extends mediodistally from the midpoint of the anterior surface to reach the proximal end of the medial distal crest. Unlike the condition in *Tyrannosaurus*, the line does not form the medial boundary of a rugose patch on the anterior surface of the distal end of femur (Brochu, 2003). A lateral intermuscular line is also present, extending along the posterolateral margin of the femur from a point level with the distal end of the lesser trochanter to the proximal end of the lateral condyle. It is most pronounced at the midshaft posterior margin, where there is a 2-cm-long, ovoid rugosity. The anterior surface of the distal femur is smooth, as in most coelurosaurians, baryonychids, coelophysoids, *Eoraptor*, and *Herrerasaurus* (Rauhut, 2003). In contrast, in many basal tetanurans, such as *Megalosaurus* (Benson, 2009), *Afrovenator* (Sereno et al., 1994; Benson, 2009), *Allosaurus* (Madsen, 1976), *Sinraptor* (Currie and

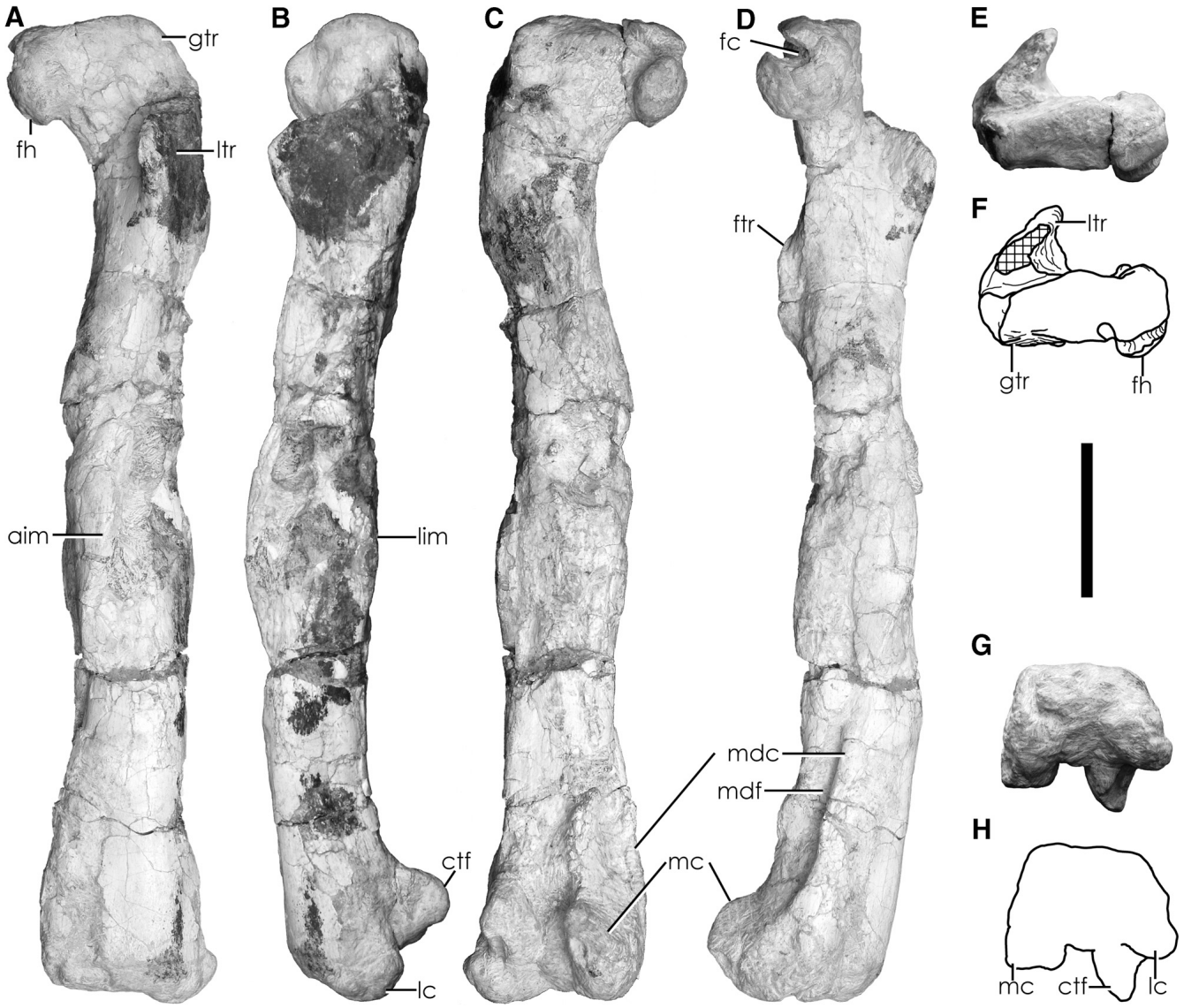

FIGURE 15. Left femur of *Zuolong salleei*. **A**, anterior; **B**, lateral; **C**, posterior; **D**, medial; **E**, **F**, proximal; **G**, **H**, distal views. **Abbreviations: aim**, anterior intermuscular line; **ctf**, crista tibiofibularis; **fc**, fovea capitis; **fh**, femoral head; **ftr**, fourth trochanter; **gtr**, greater trochanter; **lc**, lateral condyle; **lim**, lateral intermuscular line; **ltr**, lesser trochanter; **mc**, medial condyle; **mdc**, medial distal crest; **mdf**, medial distal fossa; **tfc**, fibular condyle of tibia; **II**–**IV**, metatarsals. Scale bar equals 5 cm.

Zhao, 1994), and also tyrannosauroids (Brochu, 2003; Benson, 2008a), the anterior surface of the distal end of the femur bears a large extensor groove, which is developed as a shallow, ovoid fossa located medially. The medial edge of the anterior surface of the distal end of the femur bears a medial distal crest (Benson, 2008a; also called a 'medial epicondylar crest' [Carrano et al., 2002]), a medially projecting shelf of bone that terminates at the anterolateral corner of the medial condyle. An associated fossa is located on the medial surface of the distal femur just posterior to the medial distal crest. This deep, triangular fossa extends proximally approximately one-third of the length of the medial side of the femoral shaft from its origin at the proximal end of the medial condyle. The medial distal crest is not well developed in derived coelurosaurians, and it has a sporadic distribution in other theropods. The distal left femur of the Late Jurassic basal tyrannosauroid species *Stokesosaurus langhami* (OUMNH J.3311) displays similar development of the medial distal crest; there is also a suggestion of a medial distal fossa in this taxon. In the more basal tetanurans *Allosaurus* (Madsen, 1976) and *Sinraptor* (Currie and Zhao, 1994), only a mediolaterally narrow and proximodistally short medial distal crest is present, and neither of these taxa bears a medial groove ventral to the crest. An anteroposteriorly long and mediolaterally wide crest is present in the abelisauroid *Masiakasaurus* (Carrano et al., 2002). It is unclear whether the 'expanded medial lamella' (Rauhut, 2003) seen in some theropod taxa with large extensor grooves is homologous with the medial distal crest, but the condition in *Zuolong* demonstrates that a medial distal crest can be present without an associated extensor groove. The posterior surface of the shaft of the femur is flat proximal to the distal condyles. A deep intercondylar fossa on the posterior surface of the femur between the distal condyles is continuous with a shallow popliteal fossa on the distal end of the femur. The crista tibiofibularis is longer anteroposteriorly than proximodistally, medially inset from the shaft of

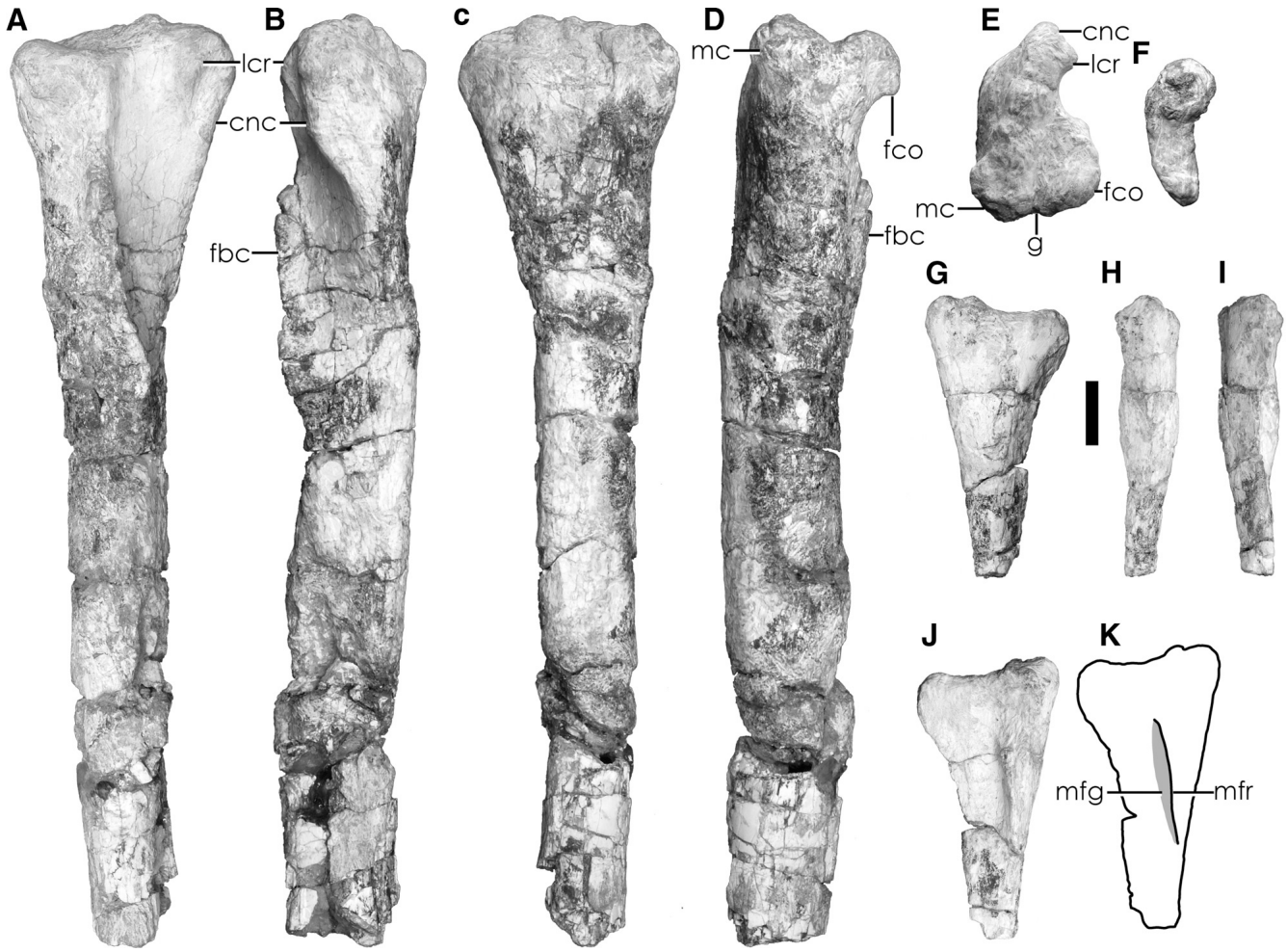

FIGURE 16. Right tibia and left fibula of *Zuolong salleei*. Right tibia in **A**, lateral; **B**, anterior; **C**, medial; **D**, posterior; **E**, proximal views. Left fibula in **F**, proximal; **G**, lateral; **H**, anterior; **I**, posterior; **J**, **K**, medial views. **Abbreviations**: **cnc**, cnemial crest; **fbc**, fibular crest; **fco**, fibular condyle; **ft**, fourth trochanter; **g**, groove; **lcr**, lateral cnemial ridge; **mc**, medial condyle; **mfg**, medial fibular groove; **mfr**, medial fibular ridge. Scale bar equals 2 cm.

the femur, and shaped like a rounded triangle in lateral view. The well-developed medial condyle is semicircular in medial view and projects distomedially from the shaft.

Tibia—The right tibia (Fig. 16A–E) is missing its distal end. The large cnemial crest is continuous with the medial edge of the proximal tibial articular surface. It originates medially and projects anterolaterally, but does not extend above the level of the proximal articular surface as in *Tyrannosaurus* (Brochu, 2003), some ornithomimosaurs (Makovicky et al., 2004b), and ceratosaurs (Tykoski and Rowe, 2004). As in a variety of theropods, the anterolateral side of the cnemial crest bears a tall, dorsoventrally oriented ridge that defines the posterior margin of the knee extensor groove (Carrano et al., 2002). The medial and fibular condyles are separated by a deep groove. The medial condyle is posteriorly rounded, whereas in *Tanycolagreus* (TPII 2000–09-29) it is posteriorly pointed. The fibular condyle extends laterally from the body of the proximal articulation and it has a deep ovoid depression on its posterior surface. The fibular crest is well developed, similar in proximodistal length to that of *Stokesosaurus langhami* (Benson, 2008a), and proximodistally long relative to those of *Allosaurus* (Madsen, 1976) and *Tyrannosaurus* (Brochu, 2003). The crest extends into the proximal end of the tibia as a low ridge that defines the posterior margin of the lateral fossa, then continues anterodistally on the lateral surface of the shaft. The crest slopes at 45° to join the tibial shaft distally. Poor preservation of the shaft makes it impossible to determine if a nutrient foramen was present posterior to the fibular crest. The tibial shaft is flat anteriorly and convex posteriorly. As preserved, the tibia is approximately 83% the length of the femur. The distal end of the preserved portion of the tibia does not exhibit any mediolateral expansion, however, indicating that a considerable portion of the length of the tibia is not preserved. In *Stokesosaurus* (OUMNH J.3311), the mediolateral expansion is limited to the distal one-eighth of the tibia. A conservative estimate of the length of the tibia of *Zuolong* would then add approximately one-eighth to the preserved length, making the tibia approximately the same length as the femur. In contrast, the tibia is 87% the length of the femur in *Allosaurus* (Madsen, 1976), 88% in *Sinraptor* (Currie and Zhao, 1994), and 87% in *Tyrannosaurus* (Brochu, 2003). In derived coelurosaurians, and especially in birds, the tibial length exceeds femoral length.

Fibula—The proximal end of the left fibula and a small portion of the proximal fibular shaft are preserved (Fig. 16F–K). In proximal view, the fibular head is shaped like an inverted comma, and it is medially concave and laterally convex. The proximal surface of the fibula bears a centrally located, saddle-shaped depression for the articulation with the fibular condyle of the femur.

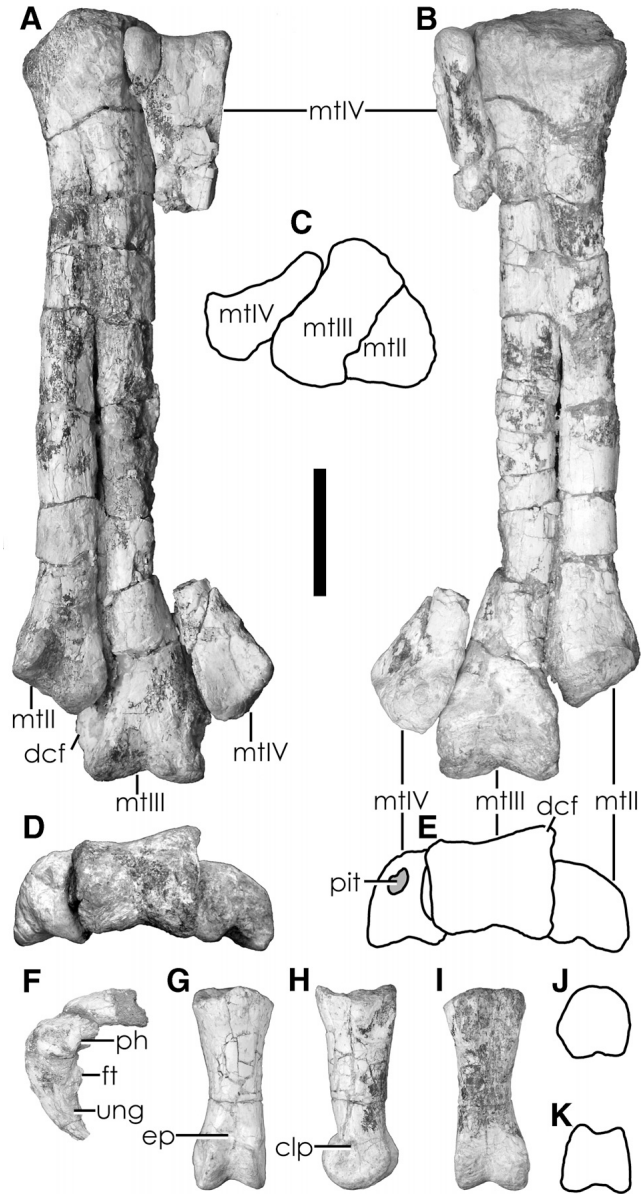

FIGURE 17. Right metatarsus and pedal bones of *Zuolong salleei*. Right metatarsus in **A**, posterior view; **B**, anterior view; **C**, proximal outline, anterior is down; **D**, **E** distal view. Pedal ungual and distal phalanx in **F**, lateral view. Proximal pedal phalanx in **G**, dorsal view; **H**, lateral; **I**, ventral view; **J**, proximal outline; **K**, distal outline. **Abbreviations**: **clp**, collateral ligament pit; **dcf**, distal condylar flange; **ep**, extensor pit; **ft**, flexor tubercle; **mt II–IV**, metatarsals II–IV; **ph**, phalanx; **pit**, pit; **ung**, ungual. Scale bar equals 2 cm.

Anterior to this depression, the proximal surface of the fibular head is convex. Posterior to this depression, the posterior end of the proximal surface is also convex, although it does not extend to the proximal level of the anterior end. The lateral surface of the fibula is convex. The medial surface bears a tall ridge along its anterior margin that forms the anterior boundary of a deep, short groove (Rauhut, 2003). The vertical ridge and its accompanying groove are well separated from the proximal end of the fibula, as in *Dilophosaurus*, *Allosaurus*, *Sinraptor*, *Ceratosaurus* (Rauhut, 2003), *Coelurus* (YPM 2010), *Ornitholestes* (AMNH 619), and *Tanycolagreus* (TPII 2000-09-29). In contrast, the medial surface of the fibula is either flat or bears an anteroposteriorly long groove (often a spoon-shaped fossa) in derived coelurosaurians (Rauhut, 2003). The small portion of the fibular shaft that is preserved is medially flat and laterally convex, yielding a D-shaped cross-section. The tubercle for insertion of the iliofibularis muscle is not preserved.

Metatarsus—Complete right metatarsals II and III and the proximal and distal ends of metatarsal IV are preserved (Fig. 17A–E). Metatarsals II and III are preserved in articulation; the proximal and distal ends of metatarsal IV are disarticulated. In proximal view, metatarsal II is triangular and metatarsal III is parallelogram-shaped, with the short edges located anteriorly and posteriorly. The proximal surface of metatarsal IV has a complex shape. It is mediolaterally widest at the convex anterior margin, tapers posteriorly, and has convex medial and concave lateral margins. There is a shallow depression on the medial edge of the anteromedial end of the proximal surface. The shafts of metatarsals II and III are nearly equal in diameter. They are anteriorly concave in lateral view. The shaft of metatarsal II bears a weakly developed, posteriorly rounded ridge along the lateral edge of its posterior surface. In many derived coelurosaurians, this ridge becomes sharply developed and extends posterolaterally. The shaft of metatarsal III is circular in cross-section proximally, but becomes more triangular in cross-section distally. The distal condyle of metatarsal II is bound to metatarsal III by matrix and the lateral condylar surface of metatarsal II is obscured. In distal view, the distal condyle of metatarsal II is not ginglymoid but comma-shaped, with the tail of the comma extending medially and the concave portion facing posteriorly. There is a shallow, circular ligament pit on the medial surface of the distal condyle. The distal condyle of metatarsal III is nearly twice the mediolateral width of distal condyles II and III. It has a well-developed ginglymus, with a shallow anterior trochlear groove and deep circular pits laterally and medially. A well-developed flange on the anteromedial edge of the distal condyle of metatarsal III extends above the lateral surface of metatarsal II. In many theropods, especially in *Coelurus* (Carpenter et al., 2005b), *Tanycolagreus* (TPII 2000-09-29), and ornithomimosaurs (e.g., *Garudimimus*; IGM 100/13-07-7), the anterior surface of the medial side of the distal condyle is expanded relative to the lateral side, but there is no flange. The distal condyle of metatarsal III projects beyond the level of the distal end of metatarsal II. The distal condyle of metatarsal IV is subtriangular in distal view and longer anteroposteriorly than mediolaterally wide. The posterior margin of the distal condyle is concave; the medial surface is also concave where it articulates with the distal shaft of metatarsal III. The lateral surface is convex, and the posterolateral margin projects posterior to the level of the posteromedial margin. There is no evidence of ligament pits on either the medial or lateral surfaces, but there is a deep pit on the distal condylar surface measuring 7 mm long and 5 mm wide. Preservation of the distal surface of the condyle is poor, but the margins of the pit are smooth and of homogeneous texture with the distal condylar surface, suggesting that the pit is an artifact of preparation or preservation.

Pes—Three pedal phalanges are preserved: the distal end of a distal phalanx in articulation with a pedal ungual (Fig. 17F) and a large proximal phalanx (Fig. 17G–K). The distal condyles of the distal phalanx are ovoid in lateral view. The pedal ungual is triangular in cross-section, with a large flexor tubercle. Symmetrical grooves on the lateral surfaces extend from the distal tip to almost to the proximal end of the bone. The proximal phalanx most likely articulated with either metatarsal II or III based on the size of its proximal articular surface. The shallowly concave proximal articular surface is subcircular and the distal end is ginglymoid. There is a deep extensor pit on the dorsal surface just proximal to the proximal end of the symmetrical distal condyles. The plantar surface is proximally flat, with a shallow groove along the

midline. There are small rugosities present medially and laterally on the proximoplantar surface.

Body Size

Body mass for *Zuolong* was estimated separately (see Supplemental Data 1 online for calculations) using the femoral length regression of Christiansen and Fariña (2004) and the skull length regression of Therrien and Henderson (2007). Using the Christiansen and Fariña regression, the body mass of *Zuolong* is estimated to have been between 50.38 and 16.22 kg. The Therrien and Henderson formula predicts a body mass of 34.25 kg, approximately at the midpoint of the estimated range using Christiansen and Fariña's (2004) formula. Body length was estimated at 3.12 m using the regression of Therrien and Henderson (2007). The calculations indicate that *Zuolong* was about half the body mass of the coeval basal tyrannosauroid *Guanlong* (Xu et al., 2006; Therrien and Henderson, 2007), and about 3% of the body mass of the contemporaneous *Sinraptor* (Therrien and Henderson, 2007).

PHYLOGENETIC ANALYSIS

We assessed the phylogenetic relationships of *Zuolong salleei* by incorporating it into a broadly sampled, species-level theropod data matrix (Supplemental Data 2 and 3). The presence of numerous coelurosaur symplesiomorphies in *Zuolong* made a priori identification to a higher taxon difficult, and based on ghost ranges for theropod lineages (Norell, 1993; Benson, 2008a; Choiniere et al., 2009), the early Late Jurassic age of the deposits at Wucaiwan permits the potential presence of representatives of many theropod groups. Therefore, we included basal theropods such as coelophysoids and ceratosaurs in our analysis and used multiple exemplar taxa (Prendini, 2001) whenever possible from theropod clades that are established in the literature. We included *Bagaraatan ostromi* (Osmólska, 1996), *Tugulusaurus faciles* (Rauhut and Xu, 2005), *Tanycolagreus topwilsoni* (Carpenter et al. 2005a), and *Aniksosaurus darwini* (Martínez and Novas, 2006) in our analysis; these four potentially basal coelurosaurian taxa have not been simultaneously considered in a published phylogenetic analysis. We did not include *Nqwebasaurus thwazi*, which was identified as a basal coelurosaur (de Klerk et al., 2000), because forthcoming work will focus on the relationships of this taxon (de Klerk et al., in preparation). The Late Cretaceous taxon *Deltadromeus* was described as a coelurosaur (Sereno et al., 1996), but was not included in this study because recent work indicates that it is a ceratosaur (Sereno et al., 2004; Carrano and Sampson, 2008).

Methods

The data matrix (Supplemental Data 2) comprises 60 taxa and 472 morphological characters. It is composed of 20 noncoelurosaurian outgroup taxa and 40 coelurosaurian ingroup taxa. It is a reduced version of a larger theropod matrix being assembled by one of us (J.N.C.) that will be presented elsewhere. Using a 'maximally diverse exemplars' approach (Prendini, 2001), we selected basal and derived taxa from each major theropod group for our analysis. We assessed whether a taxon was basal or derived based on previously published phylogenetic studies. The morphological characters in this analysis (Supplemental Data 3) are derived from data matrices published by the Theropod Working Group (ThWiG) (e.g., Norell et al., 2001; Hwang et al., 2004; Kirkland et al., 2005; Smith et al., 2007; Turner et al., 2007; Zanno et al., 2009), Rauhut's research on basal theropod relationships (2003), other published literature (e.g., Holtz, 1994, 2000; Chiappe, 1996, 2002; Novas, 1996; Forster et al., 1998; Senter, 2007; Carrano and Sampson, 2008; Longrich and Currie, 2008), and personal observations. For sources of character information for each taxon, see Supplemental Data 4.

We assembled character data in Mesquite v2.6 (Maddison and Maddison, 2008). We employed TNT v1.1 (Goloboff et al., 2003) to search for most-parsimonious trees (MPTs) using algorithms designed for large data sets (Goloboff, 2002). Searches for MPTs

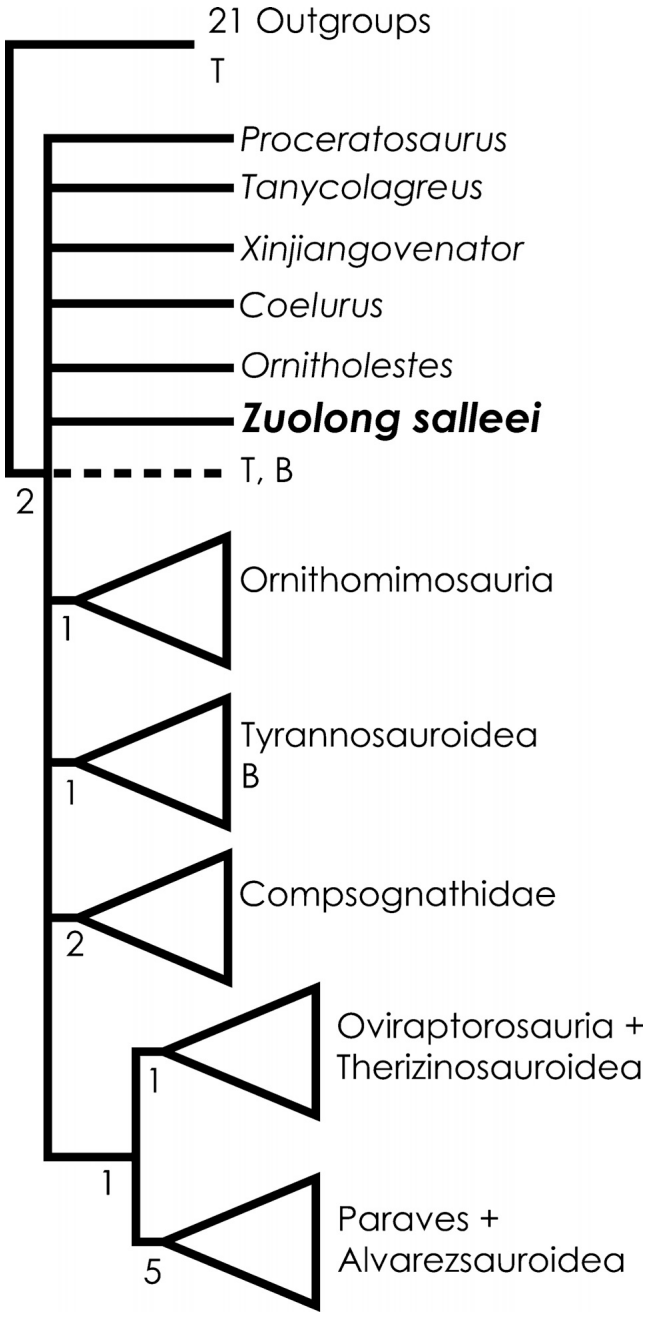

FIGURE 18. Reduced consensus cladogram of 421 most-parsimonious trees showing the relationships of *Zuolong salleei* within Coelurosauria. Outgroups and coelurosaur clades have been collapsed for summary purposes (see Supplemental Data 5 for full phylogenetic results). Taxa removed from the larger analysis were *Aniksosaurus*, *Bagaraatan*, *Stokesosaurus langhami*, and *Tugulusaurus*. Positions of these taxa in the fundamental cladograms are indicated as follows: **B**, *Bagaraatan*; **T**, *Tugulusaurus*. Numbers beneath nodes indicate decay indices. Tree length = 1732 steps; consistency index = 0.32; retention index = 0.55.

were conducted using the 'driven search' option, using Tree Drift, Tree Fusing, Ratchet, and Sectorial Searches with default settings, and stabilizing the consensus twice with a factor of 75. We submitted the 'driven search' MPTs to an additional round of TBR swapping to search for additional most parsimonious topologies. Decay indices (Bremer, 1994) and Reduced Cladistic Consensus Support Trees (Wilkinson, 1994) were calculated in TNT, saving 10,000 suboptimal trees up to 10 steps longer than the MPTs. Trees were rooted on *Eoraptor*.

Results and Discussion

Analysis of the data matrix yielded 421 MPTs of length 1732 steps, CI = 0.32, and RI = 0.55. The strict consensus of the MPTs (Supplemental Data 5) did not resolve Coelurosauria to the exclusion of outgroup taxa. Inspection of the MPTs showed this lack of ingroup resolution was due to the instability of *Tugulusaurus*, which had equally parsimonious positions within, and outside of, Coelurosauria. *Bagaaratan* was unstable within Coelurosauria in the fundamental cladograms, alternatively grouping with Ornithomimosauria and Tyrannosauroidea. We used a reduced consensus approach (Wilkinson, 1994) to calculate a consensus tree excluding these two taxa (Fig. 18).

For the following discussions, we use a modified version of the definition of Coelurosauria from Holtz et al. (2004) as all theropods more closely related to birds than to *Sinraptor dongi* and a modified version of the definition of Maniraptora from Gauthier (1986) as theropods more closely related to birds than to Ornithomimosauria.

Relationships between coelurosaurians are poorly resolved in the reduced consensus tree (Fig. 18). Although established coelurosaurian groups (e.g., Tyrannosauroidea; Holtz, 2004) were recovered as monophyletic, relationships between the nonmaniraptoran coelurosaur clades were completely unresolved. Robustness of coelurosaurian clades is generally weak, but the decay index in the reduced trees for Coelurosauria and Paraves is moderate.

Zuolong is recovered as the basal-most coelurosaurian taxon ('basal' in following discussion) in some fundamental cladograms, although in some trees it is unresolved with *Tugulusaurus* (a zero-length branch separates them) at the base of Coelurosauria. In still other trees, it was recovered at a node between Tyrannosauroidea and Ornithomimosauria ('derived' in following discussion), variably forming a sister group with *Bagaraatan* and *Proceratosaurus*. Characters supporting Coelurosauria optimize differently in the MPTs because *Zuolong* cannot be scored for some astragalar characters, and *Tugulusaurus* provides polarizations for these characters; therefore, in trees where *Tugulusaurus* is outside of Coelurosauria, astragalar characters are ambiguous for the ingroup. Furthermore, in trees where *Zuolong* is in a relatively derived position (i.e., above tyrannosauroids), some character transformations no longer optimize to the base of Coelurosauria. Coelurosaurian monophyly is supported by the following 11 characters in trees where *Zuolong* and *Tugulusaurus* are basal coelurosaurian taxa (numbers refer to characters in Supplemental Data 2 and 3): maxillary fenestra situated posterior to the rostral border of the antorbital fossa (15; also present in *Afrovenator* [Sereno et al., 1994] and *Limusaurus* [IVPP V15923]; reversed in *Incisivosaurus* [Xu et al., 2002a], *Garudimimus* [Kobayashi and Barsbold, 2005], and *Pelecanimimus* [Peréz-Moreno et al., 1994; Peréz, 2004]); dorsal border of the antorbital fossa formed by nasal and lacrimal (29; also present in *Ceratosaurus* [Madsen and Welles, 2000]; reversed in *Pelecanimimus* [Peréz-Moreno et al., 1994], *Incisivosaurus* [IVPP V13326], *Archaeopteryx* [Mayr et al., 2005], and *Confuciusornis* [Chiappe et al., 1999]); supraorbital crests on lacrimal absent (55; also absent in coelophysoids [Raath, 1977; Colbert, 1989], *Limusaurus* [Xu et al., 2009], *Majungasaurus* [Sampson and Witmer, 2007; the crest is formed by the prefrontal], *Eustreptospondylus* [Sadleir et al., 2008], and *Torvosaurus* [Britt, 1991]; present in *Tyrannosaurus* [Brochu, 2003], *Troodon* [Makovicky and Norell, 2004], and *Shuvuuia* [Chiappe et al., 1998]); D-shaped premaxillary teeth (189; absent in compsognathids [Colbert, 1989] and maniraptorans other than *Ornitholestes* [AMNH 619; Xu et al., 2002a, 2002b; Clark et al., 2004; Norell et al., 2006]); some maxillary teeth without mesial serrations (AMNH 191; does not optimize to the base of Coelurosauria when *Zuolong* is derived; reversed in tyrannosaurids [Holtz, 2004], therizinosauroids [Clark et al., 2004], and *Ornitholestes* [AMNH 619]); length of anterior cervical centra twice or more transverse width (AMNH 207; does not optimize to the base of Coelurosauria when *Zuolong* is derived; reversed in *Aniksosaurus* [Martínez and Novas, 2006], compsognathids [Peyer, 2006], and tyrannosauroids [Holtz, 2004; Xu et al., 2004] other than *Guanlong* [IVPP V14531]); amphi- to platycoelous cervical centra (211; also present in ceratosaurs [Tykoski and Rowe, 2004] and coelophysoids [Raath, 1977; Colbert, 1989; Tykoski and Rowe, 2004]; reversed in alvarezsauroids [Chiappe et al., 2002]); femur shorter than tibia (408; reversed in *Tyrannosaurus* [Brochu, 2003] and *Segnosaurus* [Clark et al., 2004]); cnemial crest proximal extent level with posterior proximal condyles of tibia (426; reversed in *Tyrannosaurus* [Brochu, 2003]); ascending process of astragalus offset from astragalar body by a pronounced groove (451; only optimizes to Coelurosauria when *Tugulusaurus* is included in that clade; also present in *Masiakasaurus* [Carrano et al., 2002]; reversed in *Segnosaurus* [Clark et al., 2004] and *Confuciusornis* [Chiappe et al., 1999]); horizontal groove across astragalar condyles absent (453; only optimizes to Coelurosauria when *Tugulusaurus* is included in that clade; also absent in *Herrerasaurus* [Novas, 1993] and coelophysoids [Tykoski and Rowe, 2004]; reversed in *Tanycolagreus* [Carpenter et al., 2005a], *Dilong* [IVPP V14242], *Coelurus* [Carpenter et al., 2005b], and *Xinjiangovenator* [IVPP V4024]).

The Middle Jurassic taxon *Proceratosaurus*, recently assigned to Tyrannosauroidea by Rauhut et al. (2009), is alternately recovered as either the sister taxon to Compsognathidae, the sister taxon to Ornithomimosauria, or as a basal tyrannosauroid in the fundamental cladograms, supporting this taxon as a basal coelurosaur (Rauhut, 2003) but suggesting that the character evidence placing this taxon with tyrannosauroids (Rauhut et al., 2009) mertis further consideration. *Aniksosaurus*, assigned to the Coelurosauria by Martínez and Novas (2006), is here recovered as a basal member of the Compsognathidae based on a fibular crest that extends from the proximal end of the fibula (433). The Late Jurassic taxon *Ornitholestes*, recovered as the basal-most maniraptoran by Turner et al. (2007), is part of a basal coelurosaurian polytomy in the reduced consensus tree. This polytomy is an artifact of the volatility of the incompletely known *Xinjiangovenator*, which forms a sister group with *Ornitholestes* in some MPTs, based on the proximal end of the tibia being of equal mediolateral width anteriorly and posteriorly (440). When *Xinjiangovenator* is removed from the consensus calculation, *Ornitholestes* is recovered as the basal-most maniraptoran. The Late Jurassic taxa *Coelurus* and *Tanycolagreus* are also recovered in a large, basal coelurosaurian polytomy. *Tanycolagreus* was recovered as a basal tyrannosauroid by Senter (2007) and at the base of Maniraptora by Rauhut et al. (2009). The phylogenetic position of the Late Cretaceous taxon *Bagaaratan*, recovered as the sister group to Maniraptora by Rauhut (2003) and Rauhut et al. (2009), and tentatively as a basal tyrannosauroid by Holtz (2004), is recovered as a member of the Tyrannosauroidea, and between Tyrannosauroidea and Ornithomimosauria in the fundamental cladograms in this analysis.

CONCLUSION

Zuolong adds to the body of knowledge of the morphology of the earliest coelurosaurians. *Zuolong* is more complete than the Jurassic basal coelurosaur taxa *Proceratosaurus*, *Tanycolagreus*, and *Coelurus* and offers further information about the morphology of the primitive coelurosaurian cranium. The ~3 m length (see Supplemental Data 1) of *Zuolong* corroborates hypotheses based on new discoveries of primitive tyrannosauroids (Xu et al., 2004; Xu et al., 2006; Benson, 2008a) that the earliest coelurosaurians were characterized by decreased body size relative to their non-coelurosaurian predecessors (Sereno, 1999; Turner et al., 2007). The character data provided by *Zuolong* help polarize some characters for the base of Coelurosauria, but more research is needed to consistently recover this group in phylogenetic analyses and to resolve relationships among basal coelurosaurians. The lack of unambiguous, uncontroverted synapomorphies for the Coelurosauria warrants caution when assigning taxa to this clade without a phylogenetic analysis.

Coelurosaurians are rare in Jurassic deposits worldwide. The discovery of *Zuolong salleei* adds to the diversity of theropods present at Wucaiwan (including as-yet unpublished specimens). Although predated by *Proceratosaurus*, and possibly by *Anchiornis* and several other relatively derived maniraptoran theropods from China, *Zuolong salleei* is one of the oldest coelurosaurians known from securely dated strata. The presence of this new taxon indicates that the theropod fauna in the earliest Late Jurassic of China was at least as diverse as that of other Late Jurassic localities, such as the Cleveland-Lloyd Dinosaur Quarry.

ACKNOWLEDGMENTS

Collection and study of this specimen were supported by NSF grants EAR 0310217, EAR 0228559, and OISE 0812234, and grants from the National Geographic Society, the National Natural Science Foundation of China, the Jurassic Foundation, the Hilmar Sallee bequest, George Washington University, and the Chinese Academy of Sciences. Research by J.N.C. was also supported by the Robert Weintraub Fellowship in Systematics and Evolution (George Washington University). We thank the crew of the Sino-American field expedition for discovering and unearthing the holotype, W. Haijun for preparing the specimen, M. Parrish and M. Ellison for providing constructive comments on illustration techniques, J. Conrad for useful discussions, M. Carrano, C. Angle, P. Barrett, D. Brinkman, B. Britt, K. Cloward, M. Getty, K. Hearst, J. Horner, S. Hutt, P. Jeffrey, W. Joyce, M. Loewen, C. Mehling, A. Milner, and R. Scheetz for access to specimens in their care, J. Georgi and J. Sipla for CT scanning the specimen, and M. Norell for use of his office space. D. Eddy and E. Schachner shared unpublished data. The manuscript was greatly improved by reviews from R. Benson, T. Carr, J. Harris, and J. A. Wilson. We thank the Willi Hennig Society for providing free access to phylogenetic software.

LITERATURE CITED

Barrett, P. M. 2009. The affinities of the enigmatic dinosaur *Eshanosaurus deguchiianus* from the Early Jurassic of Yunnan Province, People's Republic of China. Palaeontology 52:681–688.

Benson, R. B. J. 2008a. New information on *Stokesosaurus*, a tyrannosauroid (Dinosauria: Theropoda) from North America and the United Kingdom. Journal of Vertebrate Paleontology 28:732–750.

Benson, R. B. J. 2008b. A redescription of '*Megalosaurus*' *hesperis* (Dinosauria, Theropoda) from the Inferior Oolite (Bajocian, Middle Jurassic) of Dorset, United Kingdom. Zootaxa 1931:57–67.

Benson, R. B. J. 2009. A description of *Megalosaurus bucklandii* (Dinosauria: Theropoda) from the Bathonian of the UK and the relationships of Middle Jurassic theropods. Zoological Journal of the Linnean Society 158:882–935.

Bremer, K. 1994. Branch support and tree stability. Cladistics 10:295–304.

Britt, B. 1991. Theropods of the Dry Mesa Quarry (Morrison Formation, Late Jurassic), Colorado, with emphasis on the osteology of *Torvosaurus tanneri*. Brigham Young University, Geology Studies 37:1–72.

Brochu, C. A. 1996. Closure of neurocentral sutures during crocodilian ontogeny: implications for maturity assessment in fossil archosaurs. Journal of Vertebrate Paleontology 16:49–62.

Brochu, C. A. 2003. Osteology of *Tyrannosaurus rex*: insights from a nearly complete skeleton and high-resolution computed tomographic analysis of the skull. Journal of Vertebrate Paleontology 22:1–137.

Brusatte, S. L., R. B. J. Benson, T. D. Carr, T. E. Williamson, and P. C. Sereno. 2007. The systematic utility of theropod enamel wrinkles. Journal of Vertebrate Paleontology 27:1052–1056.

Carpenter, K., C. Miles, and K. Cloward. 2005a. New small theropod from the Upper Jurassic Morrison Formation of Wyoming; pp. 23–48 in K. Carpenter (ed.), The Carnivorous Dinosaurs. Indiana University Press, Bloomington and Indianapolis, Indiana.

Carpenter, K., C. Miles, J. H. Ostrom, and K. Cloward. 2005b. Redescription of the small maniraptoran theropods Ornitholestes and Coelurus from the Upper Jurassic Morrison Formation of Wyoming; pp. 49–71 in K. Carpenter (ed.), The Carnivorous Dinosaurs. Indiana University Press, Bloomington and Indianapolis, Indiana.

Carrano, M. T., and S. D. Sampson. 2008. The phylogeny of Ceratosauria (Dinosauria: Theropoda). Journal of Systematic Palaeontology 6:183–236.

Carrano, M. T., S. D. Sampson, and C. A. Forster. 2002. The osteology of *Masiakasaurus knopfleri*, a small abelisauroid (Dinosauria: Theropoda) from the Late Cretaceous of Madagascar. Journal of Vertebrate Paleontology 22:510–534.

Chiappe, L. M. 1996. Phylogenetic position of *Mononykus* from the Upper Cretaceous of the Gobi Desert. Memoirs of the Queensland Museum 39:557–582.

Chiappe, L. M. 2002. Basal bird phylogeny: problems and solutions; pp. 448–472 in L. M. Chiappe and L. M. Witmer (eds.), Mesozoic Birds: Above the Heads of Dinosaurs. University of California Press, Berkeley, California.

Chiappe, L. M., M. Norell, and J. M. Clark. 1998. The skull of a relative of the stem-group bird *Mononykus*. Nature 392:275–278.

Chiappe, L. M., M. A. Norell, and J. M. Clark. 2002. The Cretaceous, short–armed Alvarezsauridae: *Mononykus* and its kin; pp. 87–120 in L. M. Chiappe and L. M. Witmer (eds.), Mesozoic Birds: Above the Heads of Dinosaurs. University of California Press, Berkeley, California, Los Angeles, London.

Chiappe, L. M., J. Qiang, and M. A. Norell. 1999. Anatomy and systematics of the Confuciusornithidae (Theropoda: Aves) from the Late Mesozoic of northeastern China. Bulletin of the American Museum of Natural History 242:1–89.

Choiniere, J., J. Clark, X. Xu, and F. Han. 2009. A new basal alvarezsaur from the Shishugou Formation. Journal of Vertebrate Paleontology 29:77A.

Christiansen, P., and R. A. Fariña. 2004. Mass prediction in theropod dinosaurs. Historical Biology 16:85–92.

Clark, J. M., P. Altangerel, and M. A. Norell. 1994. The Skull of *Erlikosaurus andrewsi*, a Late Cretaceous "Segnosaur" (Theropoda: Therizinosauridae) from Mongolia. American Museum Novitates 3115:1–39.

Clark, J. M., T. Maryanska, and R. Barsbold. 2004. Therizinosauroidea; pp. 151–164 in D. B. Weishampel, P. Dodson, and H. Osmólska (eds.), The Dinosauria, second edition. University of California Press, Berkeley, California.

Clark, J. M., X. Xu, and C. A. Forster. 2006a. The fauna of the Middle–Upper Jurassic Shishugou Formation, Western China. Journal of Vertebrate Paleontology 26:50A.

Clark, J. M., X. Xu, D. E. Eberth, C. A. Forster, M. Machlus, S. Hemming, W. Yuan, and R. Hernandez. 2006b. The Middle-to-Late Jurassic terrestrial transition: new discoveries from the Shishugou Formation, Xinjiang, China; pp. 26–28 in 9th International Symposium, Mesozoic Terrestrial Ecosystems and Biota. University of Manchester, Manchester, U.K.

Colbert, E. H. 1989. The Triassic dinosaur *Coelophysis*. Bulletin of the Museum of Northern Arizona 53:1–61.

Coria, R. A., and P. J. Currie. 2006. A new carcharodontosaurid (Dinosauria, Theropoda) from the Upper Cretaceous of Argentina. Geodiversitas 28:71–118.

Currie, P. J., and K. Carpenter. 2000. A new specimen of *Acrocanthosaurus atokensis* from the Lower Cretaceous Antlers Formation (Lower Cretaceous: Aptian) of Oklahoma, USA. Geodiversitas 22:207–246.

Currie, P. J., and X.-J. Zhao. 1994. A new carnosaur (Dinosauria, Theropoda) from the Jurassic of Xinjiang, People's Republic of China. Canadian Journal of Earth Sciences 30:2037–2081. [*Published as 1993]

de Klerk, W. J., C. A. Forster, S. D. Sampson, A. Chinsamy, and C. F. Ross. 2000. A new coelurosaurian dinosaur from the Early Cretaceous of South Africa. Journal of Vertebrate Paleontology 20:324–332.

Dong, Z.-m. 1994. The field activities of the Sino-Canadian Dinosaur Project in China, 1987–1990. Canadian Journal of Earth Sciences 30:1997–2001. [*Published as 1993]

Duff, S. R. I. 1988. Intra-articular and para-articular defects in the pelvic limb and spine of adult male breeding turkeys. Avian Pathology 17:629–652.

Eberth, D. A., D. B. Brinkman, P.-J. Chen, F.-T. Yuan, S.-Z. Wu, G. Li, and X.-S. Cheng. 2001. Sequence stratigraphy, paleoclimate patterns, and vertebrate fossil preservation in Jurassic–Cretaceous strata of the Junggar Basin, Xinjiang Autonomous Region, People's Republic of China. Canadian Journal of Earth Sciences 38:1627–1644.

Eddy, D. 2008a. A re-analysis of the skull of *Acrocanthosaurus atokensis* (NCSM14345): implications for allosauroid morphology, phylogeny, and biogeography. Marine, Earth, and Atmospheric Sciences. North Carolina State University, Raleigh, North Carolina, 180 pp.

Eddy, D. 2008b. A re-evaluation of a well-preserved skull of *Acrocanthosaurus atokensis* supports its charcharodontosaurid affinities. Journal of Vertebrate Paleontology 28:73A.

Forster, C. A., S. D. Sampson, L. M. Chiappe, and D. W. Krause. 1998. The theropod ancestry of birds: new evidence from the Late Cretaceous of Madagascar. Science 279:1915–1918.

Gauthier, J. 1986. Saurischian monophyly and the origin of birds. Memoirs of the California Academy of Sciences 8:1–55.

Goloboff, P. A. 2002. Techniques for analyzing large datasets; pp. 70–79 in R. DeSalle, G. Giribet, and W. Wheeler (eds.), Techniques in Molecular Systematics and Evolution. Birkhauser, Basel.

Goloboff, P. A., S. Farris, and K. C. Nixon. 2003. T.N.T.: Tree Analysis Using New Technology. 1.1. The authors, Tucumán, Argentina.

Gradstein, F. M., J. G. Ogg, and A. G. Smith (eds.). 2004. A Geologic Time Scale 2004. Cambridge University Press, Cambridge, U.K., 589 pp

Grady, W. 1993. The Dinosaur Project: The Story of the Greatest Dinosaur Expedition Ever Mounted. Macfarlane Walter & Ross, Edmonton, Alberta, Canada, 261 pp.

He, H. Y., X. L. Wang, Z. H. Zhou, R. X. Zhu, F. Jin, F. Wang, X. Ding, and A. Boven. 2004. $^{40}Ar/^{39}Ar$ dating of ignimbrite from Inner Mongolia, northeastern China, indicates a post-Middle Jurassic age for the overlying Daohugou Bed. Geophysical Research Letters 31: 1–4.

Hedin, S. 1931. Across the Gobi Desert. Routledge, London, 402 pp.

Holtz, T. R., Jr. 1994. The phylogenetic position of the tyrannosauridae: implications for theropod systematics. Journal of Paleontology 68:1100–1117.

Holtz, T. R., Jr. 2000. A new phylogeny of the carnivorous dinosaurs. Gaia 15:5–61.

Holtz, T. R., Jr. 2004. Tyrannosauroidea; pp. 111–136 in D. B. Weishampel, P. Dodson, and H. Osmólska (eds.), The Dinosauria, second edition. University of California Press, Berkeley, California, and Los Angeles.

Holtz, T. R., Jr., R. E. Molnar, and P. J. Currie. 2004. Basal Tetanurae; pp. 71–110 in D. B. Weishampel, P. Dodson, and H. Osmólska (eds.), The Dinosauria, second edition. University of California Press, Berkeley, California, Los Angeles, London.

Hu, D., L. Hou, L. Zhang, and X. Xu. 2009. A pre-*Archaeopteryx* troodontid theropod from China with long feathers on the metatarsus. Nature 461:640–643.

Hwang, S. H., M. A. Norell, J. Qiang, and G. Keqin. 2004. A large compsognathid from the Early Cretaceous Yixian Formation of China. Journal of Systematic Palaeontology 2:13–30.

Irmis, R. B. 2007. Axial skeletal ontogeny in the Parasuchia (Archosauria: Pseudosuchia) and its implications for ontogenetic determination in archosaurs. Journal of Vertebrate Paleontology 27:350–361.

Kirkland, J. I., L. E. Zanno, S. D. Sampson, J. M. Clark, and D. D. DeBlieux. 2005. A primitive therizinosauroid dinosaur from the Early Cretaceous of Utah. Nature 435:84–87.

Kobayashi, Y., and R. Barsbold. 2005. Reexamination of a primitive ornithomimosaur, *Garudimimus brevipes* Barsbold, 1981 (Dinosauria: Theropoda), from the Late Cretaceous of Mongolia. Canadian Journal of Earth Sciences 42:1501–1521.

Liu, Y., Y. Liu, S.-a. Ji, and Z. Yang. 2006. U-Pb zircon age of the Daohugou Biota at Ningcheng of Inner Mongolia and comments on related issues. Chinese Science Bulletin 51:2634–2644.

Longrich, N. R., and P. J. Currie. 2008. *Albertonykus borealis*, a new alvarezsaur (Dinosauria: Theropoda) from the Early Maastrichtian of Alberta, Canada: implications for systematics and ecology of the Alvarezsauridae. Cretaceous Research 30:239–252.

Madsen, J. H., Jr. 1976. *Allosaurus fragilis*: a revised osteology. Utah Geological and Mineral Survey Bulletin 109:1–163.

Madsen, J. H., Jr., and S. P. Welles. 2000. *Ceratosaurus* (Dinosauria, Theropoda). A revised osteology. Utah Geological Survey, Miscellaneous Publication 00-2:1–80.

Maddison, W., and D. Maddison. 2008. Mesquite: A Modular System for Evolutionary Analysis. 2.6.

Makovicky, P. J., and M. A. Norell. 2004a. Troodontidae; pp. 184–195 in D. B. Weishampel, P. Dodson, and H. Osmólska (eds.), The Dinosauria, second edition. University of California Press, Berkeley, California.

Makovicky, P. J., Y. Kobayashi, and P. J. Currie. 2004b. Ornithomimosauria; pp. 137–150 in D. B. Weishampel, P. Dodson, and H. Osmólska (eds.), The Dinosauria, second edition. University of California Press, Berkeley, California.

Marsh, O. C. 1881. Principal characters of American Jurassic dinosaurs. Part V. The American Journal of Science and Arts, Series 3 21:417–423.

Martínez, R. D., and F. E. Novas. 2006. *Aniksosaurus darwini* gen. et sp. nov., a new coelurosaurian theropod from the Early Late Cretaceous of Central Patagonia, Argentina. Revista del Museo Argentino de Ciencias Naturales 8:243–259.

Mayr, G., D. S. Peters, and S. Rietschel. 2002. Petrel-like birds with a peculiar foot morphology from the Oligocene of Germany and Belgium (Aves: Procellariiformes). Journal of Vertebrate Paleontology 22:667–676.

Mayr, G., B. Pol, and D. S. Peters. 2005. A well-preserved *Archaeopteryx* specimen with theropod features. Science 310:1483–1486.

Norell, M. A. 1993. Tree-based approaches to understanding history: comments on ranks, rules and the quality of the fossil record. American Journal of Science 293A:407–417.

Norell, M. A., and P. J. Makovicky. 1997. Important features of the dromaeosaur skeleton: information from a new specimen. American Museum Novitates 3215:1–28.

Norell, M. A., and P. J. Makovicky. 2004. Dromaeosauridae; pp. 196–209 in D. B. Weishampel, P. Dodson, and H. Osmólska (eds.), The Dinosauria, second edition. University of California Press, Berkeley, California.

Norell, M. A., J. M. Clark, and P. J. Makovicky. 2001. Phylogenetic relationships among coelurosaurian theropods; pp. 49–67 in J. Gauthier and L. F. Gall (eds.), New Perspectives on the Origin and Early Evolution of Birds: Proceedings of the International Symposium in Honor of John H. Ostrom. Peabody Museum of Natural History, New Haven, Connecticut.

Norell, M. A., J. M. Clark, A. H. Turner, P. J. Makovicky, R. Barsbold, and T. Rowe. 2006. A new dromaeosaurid theropod from Ukhaa Tolgod (Omnogov, Mongolia). American Museum Novitates 3545:1–51.

Novas, F. E. 1993. New information on the systematics and postcranial skeleton of *Herrerasaurus ischigualastensis* (Theropoda: Herrerasauridae) from the Ischigualasto Formation (Upper Triassic) of Argentina. Journal of Vertebrate Paleontology 13:400–423.

Novas, F. E. 1996. Alvarezsauridae, Cretaceous basal birds from Patagonia and Mongolia. Memoirs of the Queensland Museum 39:675–702.

O'Connor, P. M. 2006. Postcranial pneumaticity: an evaluation of soft-tissue influences on the postcranial skeleton and the reconstruction

of pulmonary anatomy in archosaurs. Journal of Morphology 267:1199–1226.

O'Connor, P. M., and L. P. A. M. Claessens. 2005. Basic avian pulmonary design and flow-through ventilation in non-avian theropod dinosaurs. Nature 436:253–256.

Osmólska, H. 1996. An unusual theropod dinosaur from the Late Cretaceous Nemegt Formation of Mongolia. Acta Palaeontologica Polonica 41:1–38.

Osmólska, H., P. J. Currie, and R. Barsbold. 2004. Oviraptorosauria; pp. 165–183 in D. B. Weishampel, P. Dodson, and H. Osmólska (eds.), The Dinosauria, second edition. University of California Press, Berkeley, California, and Los Angeles.

Ostrom, J. H. 1969. Osteology of *Deinonychus antirrhopus*, an unusual theropod from the Lower Cretaceous of Montana. Peabody Museum Bulletin 30:1–165.

Peréz, B. P. 2004. *Pelecanimimus polyodon*: anatomia, systematica y paleobiología de un Ornithomimosauria (Dinosauria: Theropoda) de Las Hoyas (Cretacico Inferior; Cuenca, España). Bound volume thesis/dissertation, Facultad de Ciencias, Departmento de Biología, Unidad de Paleontología, Universidad Autónoma de Madrid, Madrid, Spain, 147 pp.

Peréz-Moreno, B. P., J. L. Sanz, A. D. Buscalloni, J. J. Moratalia, F. Ortega, and D. Rasskin–Gutman. 1994. A unique multitoothed ornithomimosaur dinosaur from the Lower Cretaceous of Spain. Nature 370:363–367.

Prendini, L. 2001. Species or supraspecific taxa as terminals in cladistic analysis? Groundplans versus exemplars revisited. Systematic Biology 50:290–300.

Peyer, K. 2006. A reconsideration of *Compsognathus* from the Upper Tithonian of Canjuers, southeastern France. Journal of Vertebrate Paleontology 26:879–896.

Raath, M. A. 1977. The anatomy of the Triassic theropod *Syntarsus rhodesiensis* (Saurischia: Podokeosauridae) and a consideration of its biology. Unpublished Ph.D. dissertation, Department of Entomology and Zoology, Rhodes University, Salisbury, Rhodesia, 233 pp.

Rauhut, O. W. M. 2003. The interrelationships and evolution of basal theropod dinosaurs, Special Papers in Palaeontology, Volume 69. The Palaeontological Association, 213 pp.

Rauhut, O. W. M., and A. Milner. 2008. Cranial anatomy and systematic position of the Middle Jurassic theropod dinosaur *Proceratosaurus* from England. Journal of Vertebrate Paleontology 28:130A.

Rauhut, O. W. M., and X. Xu. 2005. The small theropod dinosaurs *Tugulusaurus* and *Phaedrolosaurus* from the Early Cretaceous of Xinjiang, China. Journal of Vertebrate Paleontology 25:107–118.

Rauhut, O. W. M., A. C. Milner, and S. Moore-Fay. 2009. Cranial osteology and phylogenetic position of the theropod dinosaur *Proceratosaurus bradleyi* (Woodward, 1910) from the Middle Jurassic of England. Zoological Journal of the Linnean Society 158:155–195.

Sadleir, R. W., P. M. Barrett, and H. P. Powell. 2008. The anatomy and systematics of *Eustreptospondylus oxoniensis*, a theropod dinosaur from the Middle Jurassic of Oxfordshire, England. Monograph of the Palaeontographical Society Publication number 627, volume 160:1–82.

Sampson, S. D., and L. Witmer. 2007. Craniofacial anatomy of *Majungasaurus crenatissimus* (Theropoda: Abelisauridae) from the Late Cretaceous of Madagascar. Society of Vertebrate Paleontology Memoir 8 27(2, Supplement):32–102.

Senter, P. 2007. A new look at the phylogeny of Coelurosauria (Dinosauria: Theropoda). Journal of Systematic Paleontology 5:429–463.

Sereno, P. C. 1999. The evolution of dinosaurs. Science 284:2137–2147.

Sereno, P. C., J. A. Wilson, and J. L. Conrad. 2004. New dinosaurs link southern landmasses in the Mid-Cretaceous. Proceedings of the Royal Society of London, Series B 271:1335–1330.

Sereno, P. C., J. A. Wilson, H. C. E. Larsson, D. B. Duthiel, and H.-D. Sues. 1994. Early Cretaceous dinosaurs from the Sahara. Science 266:267–270.

Sereno, P. C., D. B. Duthiel, B. Gado, H. C. E. Larsson, G. H. Lyon, P. M. Magwene, C. A. Sidor, D. J. Varrichio, and J. A. Wilson. 1996. Predatory dinosaurs from the Sahara and Late Cretaceous faunal differentiation. Science 258:1137–1140.

Smith, J. B. 2005. Heterodonty in *Tyrannosaurus rex*: implications for the taxonomic and systematic utility of theropod dentitions. Journal of Vertebrate Paleontology 25:865–887.

Smith, J. B., and P. Dodson. 2003. A proposal for a standard terminology of anatomical notation and orientation in fossil vertebrate dentitions. Journal of Vertebrate Paleontology 23:1–12.

Smith, N. D., P. J. Makovicky, W. R. Hammer, and P. J. Currie. 2007. Osteology of *Cryolophosaurus ellioti* (Dinosauria: Theropoda) from the Early Jurassic of Antarctica and implications for early theropod evolution. Zoological Journal of the Linnean Society 151:377–421.

Therrien, F., and D. M. Henderson. 2007. My theropod is bigger than yours . . . or not: estimating body size from skull length in theropods. Journal of Vertebrate Paleontology 27:108–115.

Turner, A. H., D. Pol, J. A. Clarke, G. M. Erickson, and M. A. Norell. 2007. A basal dromaeosaurid and size evolution preceding avian flight. Science 317:1378–1381.

Tykoski, R. S., and T. Rowe. 2004. Ceratosauria; pp. 47–70 in D. B. Weishampel, P. Dodson, and H. Osmólska (eds.), The Dinosauria, second edition. University of California Press, Berkeley, California.

Wilkinson, M. 1994. Common cladistic information and its consensus representation: reduced Adams and reduced cladistic consensus trees and profiles. Systematic Biology 43:343–368.

Wilson, J. A. 1999. A nomenclature for vertebral laminae in sauropods and other saurischian dinosaurs. Journal of Vertebrate Paleontology 19:639–653.

Xu, K., J. Yang, M.-H. Tao, H.-D. Liang, C.-B. Zhao, R.-H. Li, H. Kong, Y. Li, C.-B. Wang, and W.-S. Peng. 2003. Jurassic System in the North of China (VII): The Stratigraphic Region of Northeast China. Petroleum Industry Press, Beijing, 261 pp.

Xu, X., and F. Zhang. 2005. A new maniraptoran dinosaur from China with long feathers on the metatarsus. Naturwissenschaften 92:173–177.

Xu, X., X. Zhao, and J. M. Clark. 2001. A new therizinosaur from the Lower Jurassic Lower Lufeng Formation of Yunnan, China. Journal of Vertebrate Paleontology 21:477–483.

Xu, X., Y.-N. Cheng, X.-L. Wang, and C.-H. Chang. 2002a. An unusual oviraptorosaurian dinosaur from China. Nature 419:291–293.

Xu, X., M. A. Norell, X.-L. Wang, P. J. Makovicky, and X.-C. Wu. 2002b. A basal troodontid from the Early Cretaceous of China. Nature 415:780–784.

Xu, X., M. A. Norell, X. Kuang, X. Wang, Q. Zhao, and C. Ji. 2004. Basal tyrannosauroids from China and evidence for protofeathers in tyrannosauroids. Nature 431:680–684.

Xu, X., J. M. Clark, C. A. Forster, M. A. Norell, G. M. Erickson, D. A. Eberth, C. Ji, and Q. Zhao. 2006. A basal tyrannosauroid dinosaur from the Late Jurassic of China. Nature 439:715–718.

Xu, X., J. M. Clark, J. Mo, J. Choiniere, C. A. Forster, G. M. Erickson, D. W. E. Hone, C. Sullivan, D. A. Eberth, S. Nesbitt, Q. Zhao, R. Hernandez, C.-k. Jia, F.-l. Han, and Y. Guo. 2009. A Jurassic ceratosaur from China helps clarify avian digital homologies. Nature 459:940–944.

Young, C. C. 1937. A new dinosaurian from Sinkiang. Paleontologica Sinica Series C 7:1–53.

Zanno, L. E., D. B. Gillette, L. B. Albright, and A. L. Titus. 2009. A new North American therizinosaurid and the role of herbivory in 'predatory' dinosaur evolution. Proceedings of the Royal Society of London, Series B 276:3505–3511.

Zhang, F, Z. Zhou, X. Xu, and X. Wang. 2002. A juvenile coelurosaurian theropod from China indicates arboreal habits. Naturwissenschaften 89:394–398.

Zhang, F, Z. Zhou, X. Xu, Wang, X., and C. Sullivan. 2008. A bizarre Jurassic maniraptoran from China with elongate ribbon-like feathers. Nature 455:1105–1108.

Zhao, X.-J., and P. J. Currie. 1994. A large crested theropod from the Jurassic of Xinjiang, People's Republic of China. Canadian Journal of Earth Sciences 30:2027–2036. [*Published as 1993]

Submitted January 21, 2010; accepted May 27, 2010.